



Article

# The Role of $K_V7.3$ in Regulating Osteoblast Maturation and Mineralization

Ji Eun Yang, Min Seok Song, Yiming Shen, Pan Dong Ryu and So Yeong Lee \*

Laboratory of Veterinary Pharmacology, College of Veterinary Medicine and Research Institute for Veterinary Science, Seoul National University, 1 Gwanak-ro, Gwanak-gu, Seoul 151-742, Korea; didwldms@snu.ac.kr (J.E.Y.); gan14@snu.ac.kr (M.S.S.); sym1987@snu.ac.kr (Y.S.); pdryu@snu.ac.kr (P.D.R.)

\* Correspondence: leeso@snu.ac.kr; Tel.: +82-2-880-1283; Fax: +82-2-879-0378

Academic Editor: Charles J. Malemud

Received: 2 March 2016; Accepted: 10 March 2016; Published: 18 March 2016

**Abstract:** KCNQ ( $K_V7$ ) channels are voltage-gated potassium ( $K_V$ ) channels, and the function of  $K_V7$  channels in muscles, neurons, and sensory cells is well established. We confirmed that overall blockade of  $K_V$  channels with tetraethylammonium augmented the mineralization of bone-marrow-derived human mesenchymal stem cells during osteogenic differentiation, and we determined that  $K_V7.3$  was expressed in MG-63 and Saos-2 cells at the mRNA and protein levels. In addition, functional  $K_V7$  currents were detected in MG-63 cells. Inhibition of  $K_V7.3$  by linopirdine or XE991 increased the matrix mineralization during osteoblast differentiation. This was confirmed by alkaline phosphatase, osteocalcin, and osterix in MG-63 cells, whereas the expression of Runx2 showed no significant change. The extracellular glutamate secreted by osteoblasts was also measured to investigate its effect on MG-63 osteoblast differentiation. Blockade of  $K_V7.3$  promoted the release of glutamate via the phosphorylation of extracellular signal-regulated kinase 1/2-mediated upregulation of synapsin, and induced the deposition of type 1 collagen. However, activation of  $K_V7.3$  by flupirtine did not produce notable changes in matrix mineralization during osteoblast differentiation. These results suggest that  $K_V7.3$  could be a novel regulator in osteoblast differentiation.

**Keywords:** KCNQ channels; differentiation; matrix mineralization; glutamate

## 1. Introduction

Voltage-gated  $K^+$  ( $K_V$ ) channels are one of the largest gene families among the  $K^+$  channel groups.  $K_V$  channels are known for regulating cellular electrophysiological properties in excitable cells such as neurons [1–3] and muscle cells [4–6]. In neurons and cardiac muscle cells,  $K_V$  channels repolarize the cell membrane after the action potential; in association with this action,  $K_V$  channels modulate the firing rate of the action potential, membrane stabilization, and neurotransmission [7,8].  $K_V$  channels also serve as regulators in non-excitable cells. Specific  $K_V$  channels are expressed in most malignant cells, including those in leukemia [9], breast cancer [10–13], colon cancer [14–17], and gastric cancer [18], and they regulate cell proliferation [11,12,14,17,19–23], migration [16,24,25], and differentiation [22,26,27].  $K_V$  channels may also affect cell volume [13,28] and cell signaling [29], leading to diverse cellular activities.

KCNQ channels are  $K_V$  channel members, also known as  $K_V7$  channels, comprising  $K_V7.1$  through  $K_V7.5$ . These channels are widely distributed throughout various tissues [30].  $K_V7.1$  was first identified in the heart and has been well-characterized in cardiac muscle cells [28,30]; it is also present in the inner ear epithelium [31], lung [32], and gastrointestinal tract [33].  $K_V7.2$  and  $K_V7.3$  are mainly expressed in the central nervous system [27,34,35], usually forming a  $K_V7.2/7.3$  heterotetramer, which contributes M-current [36].  $K_V7.4$  is present in skeletal muscle cells [22,37] and outer hair cell membrane [30], and

K<sub>V</sub>7.5 is widely distributed in the brain [38]. Previous studies have determined the physiological role of KCNQ channels in cell proliferation, differentiation [17,22,23,37], and survival [22].

Bone is a complicated organ that continuously undergoes formative and resorptive activities, driven by osteoblasts and osteoclasts [39,40]. The development of bone depends on various extracellular signals and transcription factors to maintain its structure and homeostasis, so the microenvironment is significant for bone physiology. Sequential expressions of regulatory signals are necessary for bone cell differentiation. First, cytokines, such as bone morphogenic protein and transforming growth factor- $\beta$  [41–43], and transcription factors, such as Runx2 [42,44,45], are required to transform a pluripotent stem cell into an osteoprogenitor cell and then into a pre-osteoblast. The pre-osteoblast then undergoes matrix mineralization, a distinctive step in osteoblast differentiation. At this stage, osteoblast-derived factors, such as osteocalcin, alkaline phosphatase, collagens, and bone sialoproteins [44,46], mediate the initiation and formation of extracellular matrix mineralization by vesicle-mediated exocytosis [47].

K<sub>V</sub>7 channels have been reported to regulate cell differentiation. For example, K<sub>V</sub>7.4 plays a role in skeletal muscle cell development [22,37], and another report indicated that K<sub>V</sub>7.2/7.3 was involved in neuronal differentiation through synaptic vesicle protein-mediated endo/exocytosis of neurotransmitters [27]. M-current by K<sub>V</sub>7 channels is controlled by multiple factors, including intracellular Ca<sup>2+</sup> [30,48–52]. Considering the fact that Ca<sup>2+</sup> is pivotal for bone homeostasis and that KCNQ channels modulate vesicular exocytosis, we explored the potential role of KCNQ channels in bone differentiation, focusing on biological mineralization of the bone matrix. First, the overall effect of K<sub>V</sub> channels on human mesenchymal stem cell (hMSC) osteogenic differentiation was confirmed. We then focused on K<sub>V</sub>7 channel expression in osteoblast-like cells, and developed the tentative theory that K<sub>V</sub>7 channels, or at least K<sub>V</sub>7.3, may play potential roles in osteoblast differentiation through glutamatergic communication, especially for matrix maturation and mineralization.

## 2. Results

### 2.1. Effects of Tetraethylammonium, A Non-Selective Potassium Channel Blocker, on Human Mesenchymal Stem Cell Osteogenic Differentiation

Bone marrow-derived human mesenchymal stem cells (hMSCs) were differentiated into the osteoblastic lineage when treated with osteogenic-induction medium (OM) for 16 days. Extracellular calcium deposits were identified via Alizarin Red S staining. The hMSCs in OM produced calcium deposits in the extracellular matrix, which represented the color red, while the cells incubated in the growth medium (GM) did not show calcium deposits (Figure 1A). The optical density (OD) values also showed that only the OM-treated hMSCs were differentiated into the osteogenic lineage (Figure 1B).

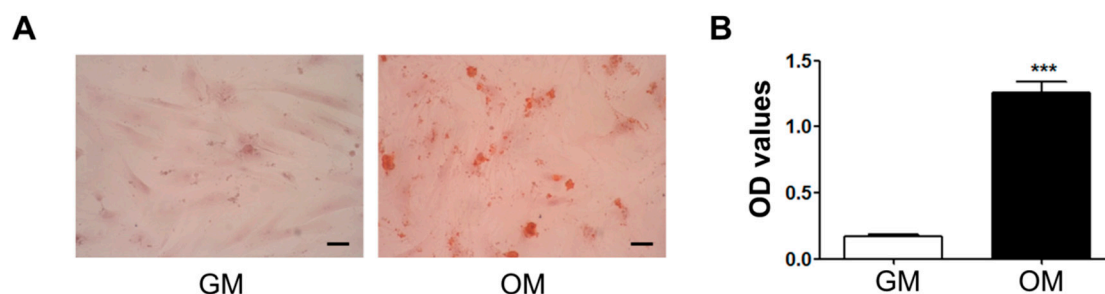
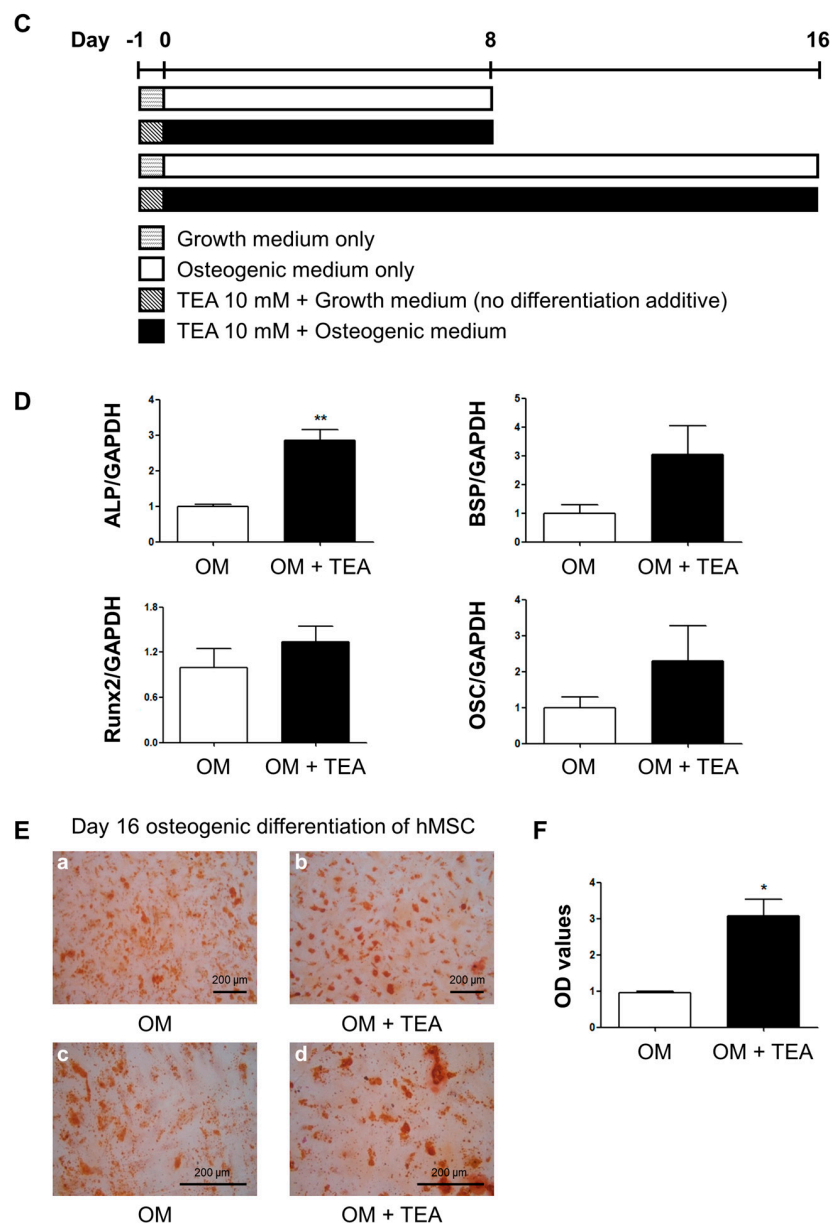


Figure 1. Cont.



**Figure 1.** Regulation of human mesenchymal stem cell (hMSC) osteogenic differentiation by tetraethylammonium (TEA). Matrix mineralization was evaluated via Alizarin Red S staining. (A) Differentiated hMSCs in osteogenic-induction medium (OM) produced calcium deposits and were dyed red (right), while the cells cultured in growth medium (GM) were not stained (left). The hMSCs were differentiated for 10 days; (B) The OD values for Alizarin Red S staining showed that hMSCs cultured in OM had a greater calcium content than those in GM; (C) Scheme for the protocol of TEA treatment during hMSC osteogenic differentiation. Cells were pre-incubated with 10 mM TEA for 1 day without any differentiation additives. OM containing TEA was used to induce hMSC osteogenic differentiation; (D) The mRNA expressions of osteogenic differentiation markers were analyzed with qRT-PCR at day 8 of osteogenic differentiation. The mRNA expression of ALP was significantly increased. The expressions of BSP and OSC tended to increase, although not statistically significantly. There was no significant change in Runx2 expression; (E) Alizarin Red S staining demonstrated that hMSC osteogenic differentiation was increased by TEA. The hMSCs treated with TEA produced greater calcium contents; (F) The OD values demonstrated that TEA increased hMSC osteogenic differentiation. The OD values were normalized with the Alamar Blue Assay to consider remained cell numbers ( $n = 3$ ). The data are presented as mean  $\pm$  SEM. \*  $p < 0.05$ ; \*\*  $p < 0.01$ ; and \*\*\*  $p < 0.005$  compared to controls. Scale bar represents 200  $\mu\text{m}$ . ALP: alkaline phosphatase; BSP: bone sialoprotein; OSC: osteocalcin; OD: optical density.

To investigate the overall effect of  $K_V$  channels on hMSC osteogenic differentiation, a non-selective  $K_V$  channel blocker, tetraethylammonium (TEA), was applied to hMSCs during differentiation. The protocol is presented in Figure 1C. Several osteoblast gene markers, such as alkaline phosphatase (ALP), bone sialoprotein (BSP), Runx2, and osteocalcin (OSC), were analyzed with quantitative RT-PCR (qRT-PCR) at day 8 of osteogenic differentiation. ALP gene expression was augmented by TEA compared to the controls (Figure 1D). TEA increased hMSC mineralization, and Alizarin Red S staining demonstrated that hMSCs treated with TEA produced more calcium deposits per unit area (Figure 1E), although fewer cells remained because of the cytotoxic effect of TEA. An Alamar Blue assay was used to determine the cytotoxicity of TEA on hMSCs (data not shown). The OD values in Figure 1F were normalized by the result of the Alamar Blue assay.

## 2.2. Expression of $K_V7$ Channels in Osteoblast-Like Cell Lines, MG-63 and Saos-2

To identify the effect of  $K_V$  channels on osteogenic properties, the mRNA expression of KCNQ gene subfamilies, including  $K_V7.1$ ,  $K_V7.2$ ,  $K_V7.3$ ,  $K_V7.4$ , and  $K_V7.5$  in MG-63 and Saos-2 cells, was analyzed using RT-PCR. While all  $K_V7$  channel subtypes were present in the MG-63 cells (Figure 2A),  $K_V7.3$  and  $K_V7.5$  were expressed in the Saos-2 cells (Figure 2B).

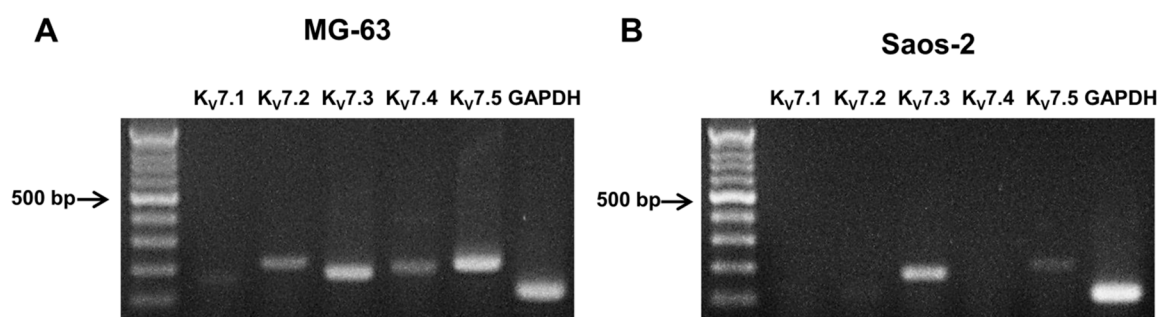


**Figure 2.** RT-PCR analysis of the  $K_V7$  channels in osteoblast-like cells. The PCR products using cDNA from the MG-63 (A) and Saos-2 cells (B) were electrophoresed in a 1.6% agarose gel ( $n = 5$ ).

## 2.3. mRNA and Protein Expression and Functional Activities of $K_V7$ Channels during Osteoblastic Differentiation

In RT-PCR analysis, we confirmed that MG-63 cells strongly express  $K_V7.2$ ,  $K_V7.3$ , and  $K_V7.5$  in MG-63 and  $K_V7.3$  in Saos-2 cells. We therefore examined the expression levels of these channels during osteoblast differentiation using qRT-PCR. These results demonstrated that the mRNA levels of  $K_V7.2$  and  $K_V7.5$  were not significantly changed during osteoblast differentiation in MG-63 cells (Figure 3A). In contrast, the mRNA expression of  $K_V7.3$  significantly decreased 8 h after osteoblast induction; however, at day 14, the mRNA level of  $K_V7.3$  showed a substantial increase (Figure 3A). Similarly, in Saos-2 cells, while the  $K_V7.3$  transcripts significantly decreased 1 h after osteoblast induction, the  $K_V7.3$  transcripts level increased considerably at day 14 of osteoblast differentiation (Figure 3B). We also investigated the changes in  $K_V7.3$  protein expression, and the western blot analysis illustrated that  $K_V7.3$  proteins increased at days 4 and 14 after osteoblast induction in the MG-63 and Saos-2 cells (Figure 3C,D).

Whole-cell patch clamp recordings were performed on early osteoblastic differentiation before extracellular matrix production began. These results showed that functional  $K_V7.3$  currents were present in MG-63 cells at days 0 and 2 of osteoblast differentiation (Figure 4A,C). Voltage-current relationships illustrated that XE991 significantly inhibited  $K_V7.3$  currents (Figure 4B,D). Normalized XE991-sensitive  $K_V7.3$  currents at days 2 and 3 were increased by 54.03% and 54.52%, respectively, but not statistically significant (Figure 4E).

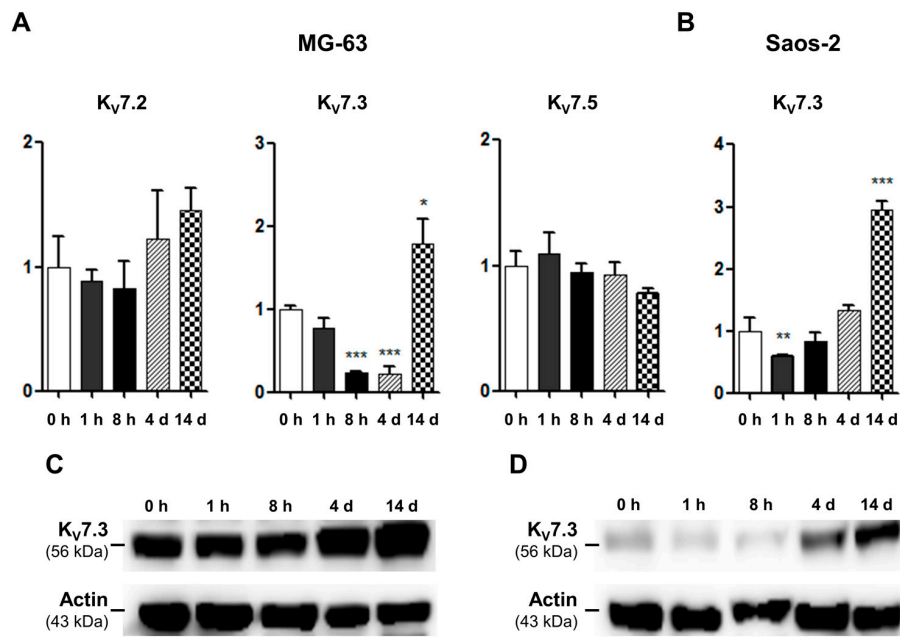


**Figure 3.** Changes in K<sub>v</sub>7 channel expression during osteoblastic differentiation. The relative expression levels of K<sub>v</sub>7.2, K<sub>v</sub>7.3, and K<sub>v</sub>7.5 during osteoblast differentiation were analyzed by qRT-PCR. (A) In MG-63 cells, mRNA expressions of K<sub>v</sub>7.2 and K<sub>v</sub>7.5 were not significantly changed ( $n = 3$ ). However, K<sub>v</sub>7.3 transcripts decreased for 4 days after osteoblast induction, whereas, at day 14, the K<sub>v</sub>7.3 mRNA level was considerably increased ( $n = 4$ ); (B) In Saos-2 cells, mRNA expression of K<sub>v</sub>7.3 was reduced 1 h after osteoblast induction, but was significantly augmented at day 14 ( $n = 4$ ); (C,D) The expression of K<sub>v</sub>7.3 proteins was increased at day 4 of osteoblast induction ( $n = 3$ ). Data are presented as mean  $\pm$  SEM. \*  $p < 0.05$ ; \*\*  $p < 0.01$ ; and \*\*\*  $p < 0.005$ . d: day.

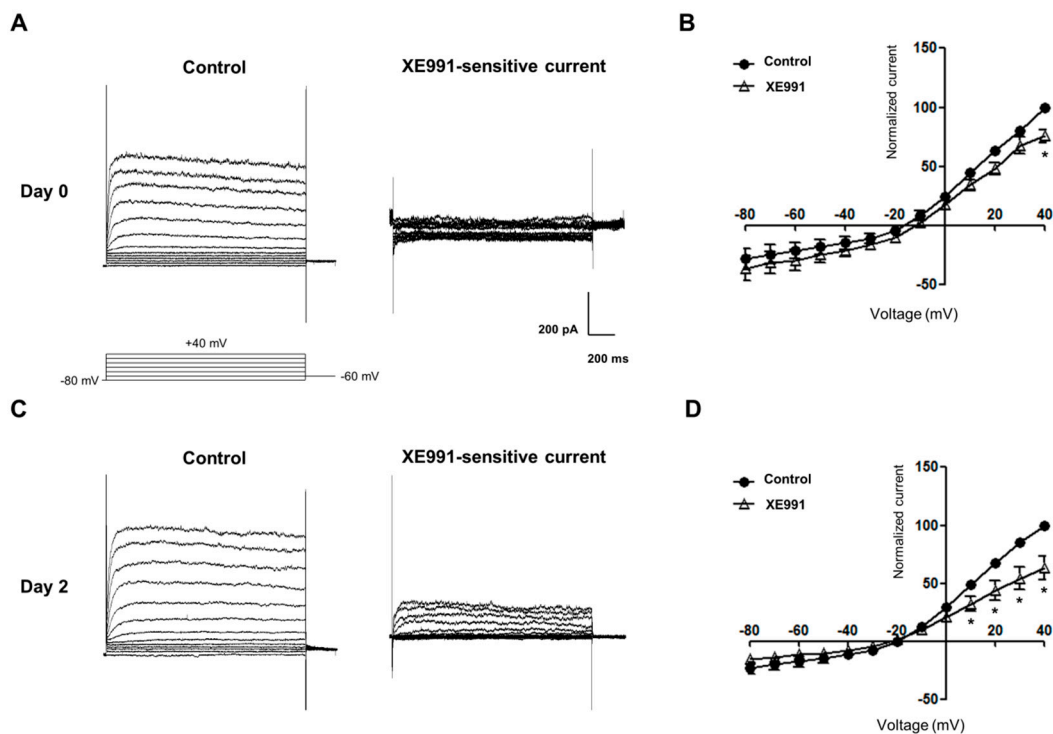


**Figure 4.** Cont.

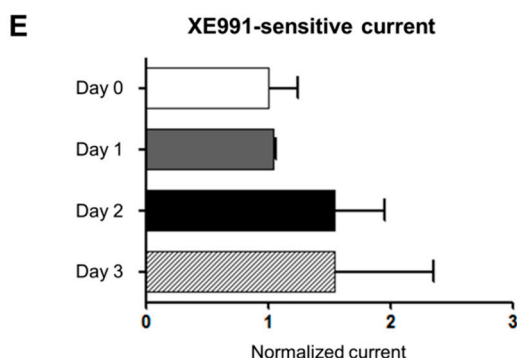


**Figure 4.** Functional characteristics of  $K_V7.3$  channel in MG-63 cells during osteoblast differentiation. (A) Representative current responses to depolarizing steps observed at day 0 of undifferentiated MG-63 cells. XE991-sensitive currents were obtained by the subtraction of the currents in controls from in the presence of XE991 (50  $\mu$ M); (B) Current-voltage relationships in controls and in the presence of XE991 at day 0 ( $n = 3$ ); (C) Representative current responses to depolarizing steps observed at day 2 of osteoblastic differentiation; (D) Current-voltage relationships in controls and in the presence of XE991 at day 2 ( $n = 4$ ); (E) XE991-sensitive currents at days 0–4 were normalized by mean current value at day 0. At day 1 of osteoblast differentiation, normalized XE991-sensitive currents had no significant change. At days 2 and 3, the  $K_V7.3$  currents were increased, but not statistically significant. Data are presented as mean  $\pm$  SEM. \*  $p < 0.05$ .

To confirm the effect of  $K_V7.3$  modulators on cell viability, the MTT assay was performed on MG-63 cells. A  $K_V7$  opener, flupirtine (30  $\mu$ M), and  $K_V7.3$  blockers, linopirdine (30  $\mu$ M) and XE991 (10  $\mu$ M) were used. Although treatment with flupirtine attenuated cell viability at 24 h, overall cell viability was not significantly affected by treatment with flupirtine, linopirdine, and XE991 at 24 and 48 h. However, at 72 h, the  $K_V7$  opener and  $K_V7.3$  blocker-treated groups showed significant decreases in cell viability in GM (Figure 5A). To further understand the effect on cell viability during osteoblastic differentiation, we cultured MG-63 cells in OM under the same conditions, and then performed MTT assays. The results indicated that although linopirdine reduced cell proliferation at 24 h, there was no significant change in overall cell viability, when treated with OM containing the  $K_V7.3$  blockers or the  $K_V7$  opener (Figure 5B).

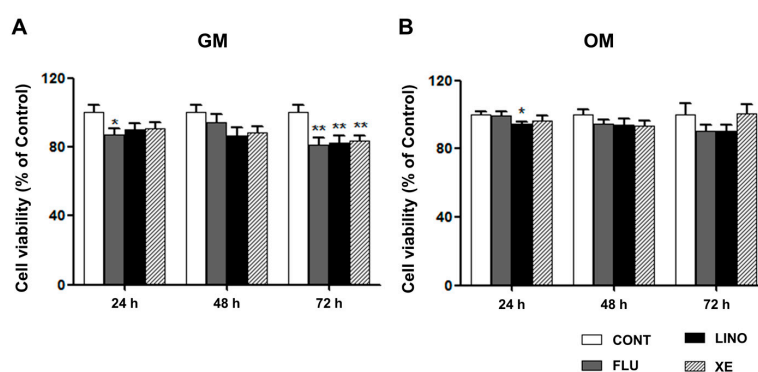


**Figure 5.** Effect of flupirtine, linopirdine, and XE991 on MG-63 cell viability. The MTT assay was performed on MG-63 cells. (A) MG-63 cells were incubated in growth medium (GM) with 30  $\mu$ M of flupirtine, 30  $\mu$ M of linopirdine, and 10  $\mu$ M of XE991. At 72 h, linopirdine, XE991, and flupirtine caused notable decreases in cell viability ( $n = 16$ ); (B) MG-63 cells were cultured in osteoblast-induction medium (OM) with 30  $\mu$ M of flupirtine, 30  $\mu$ M of linopirdine, and 10  $\mu$ M of XE991. The cell viability was not significantly influenced by OM containing linopirdine, XE991, or flupirtine for 72 h of treatment ( $n = 16$ ). The values are presented as mean  $\pm$  SEM. \*  $p < 0.05$  and \*\*  $p < 0.01$ . CONT: non-treated controls; FLU: flupirtine; LINO: linopirdine; XE: XE991.

#### 2.4. Regulation of Mineralization by $K_V7.3$ Blockers or the $K_V7$ Opener in MG-63 and Saos-2 Cells

We confirmed the effect of the  $K_V7.3$  channel on calcium deposition in the extracellular matrix using Alizarin Red S staining. The  $K_V7.3$  blockade by linopirdine (30  $\mu\text{M}$ ) or XE991 (10  $\mu\text{M}$ ) noticeably increased mineralization in MG-63 cells. On the other hand,  $K_V7$  activation by flupirtine (30  $\mu\text{M}$ ) did not show an effect on mineralization (Figure 6A,B). These experiments were conducted with additional osteoblast-like Saos-2 cells to examine the effect of blocking  $K_V7$  channels on mineralization. The results showed that linopirdine (30  $\mu\text{M}$ ) and XE991 (10  $\mu\text{M}$ ) significantly promoted mineralization, whereas flupirtine (30  $\mu\text{M}$ ) attenuated the extent of calcium deposits of Saos-2 cells (Figure 6C,D). Therefore, the inhibition of  $K_V7.3$  channels augmented mineralization, facilitating osteoblast differentiation.

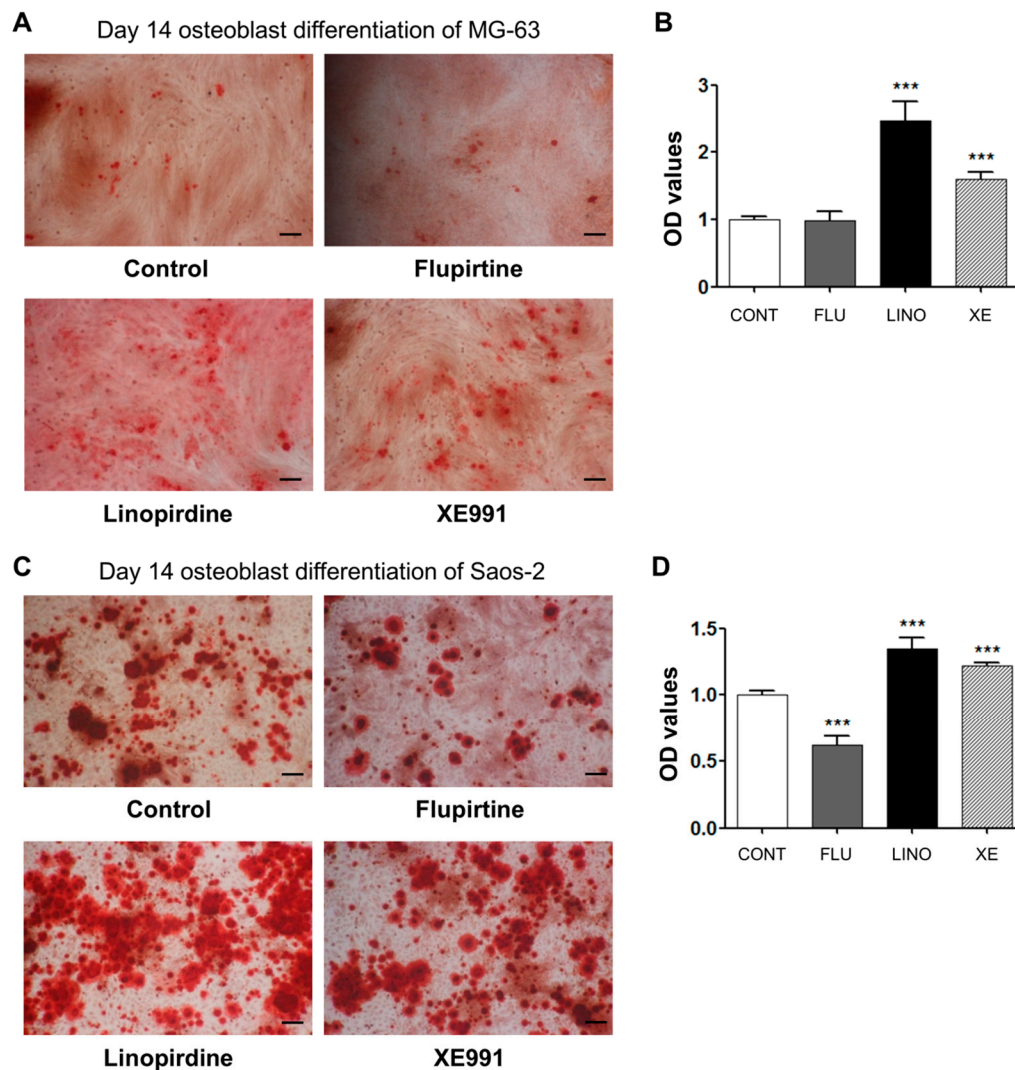


**Figure 6.** Regulation of osteoblastic differentiation by  $K_V7$  channel in MG-63 and Saos-2 cells. (A) Alizarin Red S staining data showed that 30  $\mu\text{M}$  of linopirdine and 10  $\mu\text{M}$  of XE991 augmented mineralization in the extracellular matrix in MG-63 cells ( $n = 10$ ). There was no significant change in the mineralized matrix with 30  $\mu\text{M}$  of flupirtine ( $n = 3$ ); (B) The OD values demonstrated that linopirdine and XE991 increased the amount of calcium deposits; (C) Alizarin Red S staining illustrated that mineralization of Saos-2 cells was increased with 30  $\mu\text{M}$  of linopirdine and 10  $\mu\text{M}$  of XE991 ( $n = 8$ ), while 30  $\mu\text{M}$  of flupirtine reduced the amount of calcium deposits ( $n = 7$ ); (D) The OD values are shown parallel to Alizarin Red S staining results. Data are presented as mean  $\pm$  SEM. \*\*\*  $p < 0.005$ . Scale bar represents 100  $\mu\text{m}$ . CONT: non-treated controls; FLU: flupirtine; LINO: linopirdine; XE: XE991; OD: optical density.

### 2.5. Regulation of Osteoblast Differentiation Markers by $K_V7$ Channels in MG-63 Cells

We examined the mRNA expression of ALP, OSC, Runx2, and osterix using qRT-PCR. Linopirdine (30  $\mu$ M) and XE991 (10  $\mu$ M) significantly increased ALP gene expression at days 7 and 10 of osteoblast induction, whereas  $K_V7$  activation by flupirtine (30  $\mu$ M) attenuated the expression of ALP (Figure 7A). Additionally, the mRNA expression of OSC was increased by linopirdine and XE991 at days 7 and 10, respectively, while flupirtine showed no significant effect on OSC expression (Figure 7B). We also identified the expression of Runx2 and osterix, which are known as essential transcription factors that promote hMSC differentiation into osteogenic lineages. Although the level of Runx2 was decreased by linopirdine at day 10, linopirdine and XE991 did not produce changes in Runx2 levels through overall osteoblast differentiation (Figure 7C). However, at day 10, blockade of  $K_V7.3$  by linopirdine and XE991 augmented the mRNA expression of osterix; flupirtine did not result in significant changes (Figure 7D).

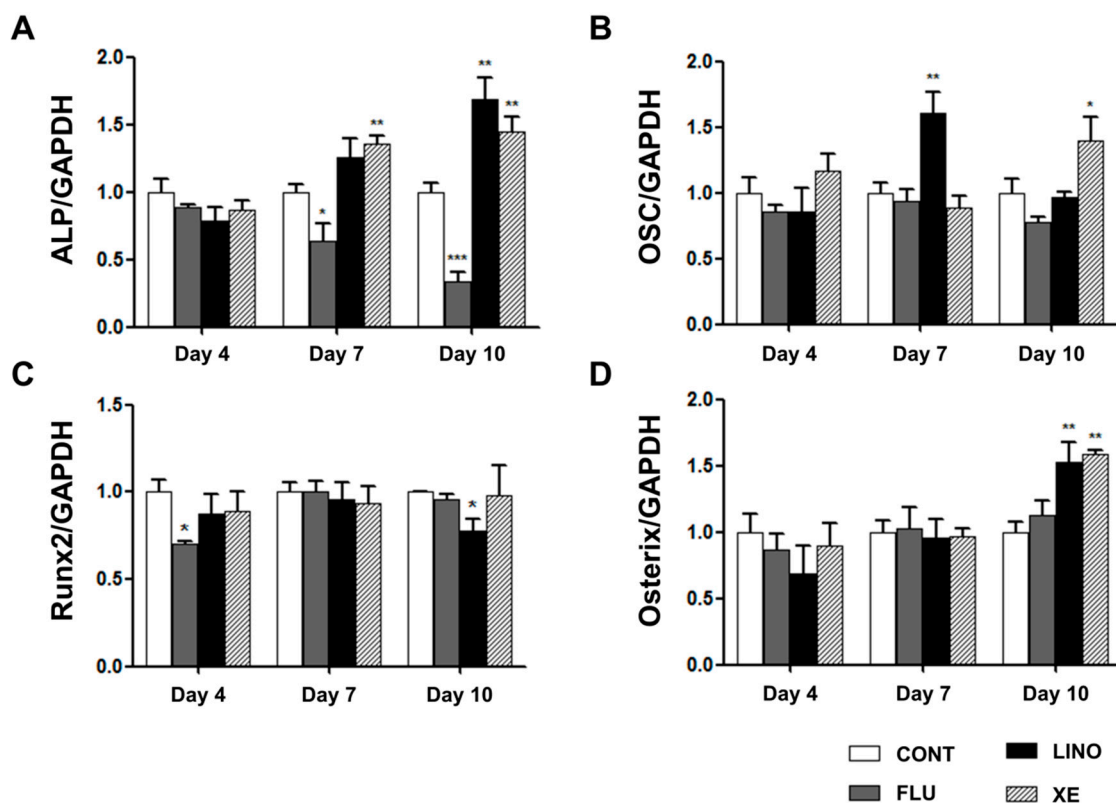


**Figure 7.** mRNA expression of osteoblastic differentiation markers in MG-63 cells. The relative mRNA expression levels of osteoblastic differentiation markers, ALP, OSC, Runx2, and osterix, were measured with qRT-PCR and normalized against glyceraldehyde 3-phosphate dehydrogenase (GAPDH) expression. (A) While linopirdine (30  $\mu$ M) and XE991 (10  $\mu$ M) increased ALP mRNA expression at days 7 and 10 of osteoblastic induction, flupirtine (30  $\mu$ M) decreased ALP mRNA expression at days 7 and 10 ( $n = 3-7$ ); (B) The mRNA expression level of OSC was increased by linopirdine or XE991 at days 7 and 10, respectively ( $n = 3-7$ ); (C) mRNA expression of Runx2 was decreased by flupirtine at day 4 and by linopirdine at day 10 ( $n = 3$ ); (D) Osterix gene expression was increased by linopirdine and by XE991 at day 10 of osteoblastic induction ( $n = 3-7$ ). The values are presented as mean  $\pm$  SEM. \*  $p < 0.05$ ; \*\*  $p < 0.01$ ; and \*\*\*  $p < 0.005$ . ALP: alkaline phosphatase; OSC: osteocalcin; CONT: non-treated controls; FLU: flupirtine; LINO: linopirdine; XE: XE991.

## 2.6. Effect of $K_V7$ Channel Modulations on Synaptic Vesicle-Related Synapsin and the Mitogen-Activated Protein Kinase (MAPK) Signaling Pathway

In previous experiments, we identified that  $K_V7.3$  inhibition using linopirdine or XE991 increased mineralization during osteoblast differentiation. Focusing on these results, synapsin and extracellular signal-regulated kinase 1/2 (ERK1/2) expressions were examined to verify whether  $K_V7$  channels were involved in vesicular exocytosis during matrix mineralization. First, the expression of the synaptic vesicle-related protein synapsin was increased by the  $K_V7.3$  blockers, linopirdine (30  $\mu$ M) and XE991 (10  $\mu$ M), whereas  $K_V7$  activation by flupirtine (30  $\mu$ M) had no effect (Figure 8). In the same manner, while inhibition of  $K_V7.3$  by linopirdine or XE991 increased the ERK1/2 phosphorylation (p-ERK1/2),  $K_V7$  activation by flupirtine resulted in no significant changes to p-ERK1/2 levels. On the other hand, at day 14, blockade by linopirdine or XE991 produced no increase in p-ERK1/2, but flupirtine increased its expression (Figure 9).

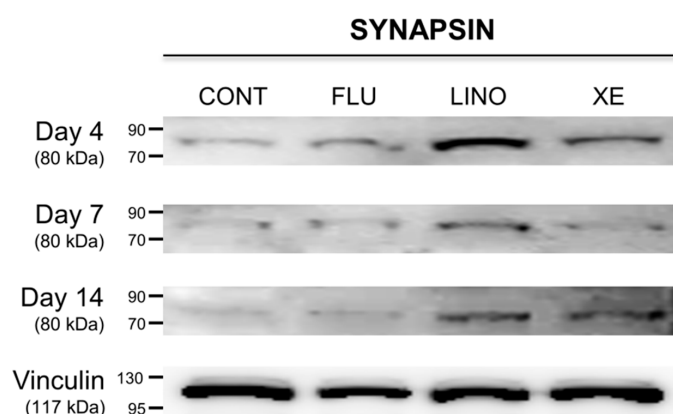


**Figure 8.** Regulation of synaptic vesicle-related protein, synapsin, by  $K_V7.3$  channel in MG-63 cells. Western blot analysis showed that  $K_V7.3$  blockade by linopirdine (30  $\mu$ M) or XE991 (10  $\mu$ M) increased synapsin expression during osteoblast differentiation. However,  $K_V7$  activation by flupirtine (30  $\mu$ M) had no significant effect on the protein expression of synapsin ( $n = 3$ ). Vinculin is used as a loading control for Western blot analysis. CONT: non-treated controls; FLU: flupirtine; LINO: linopirdine; XE: XE991.

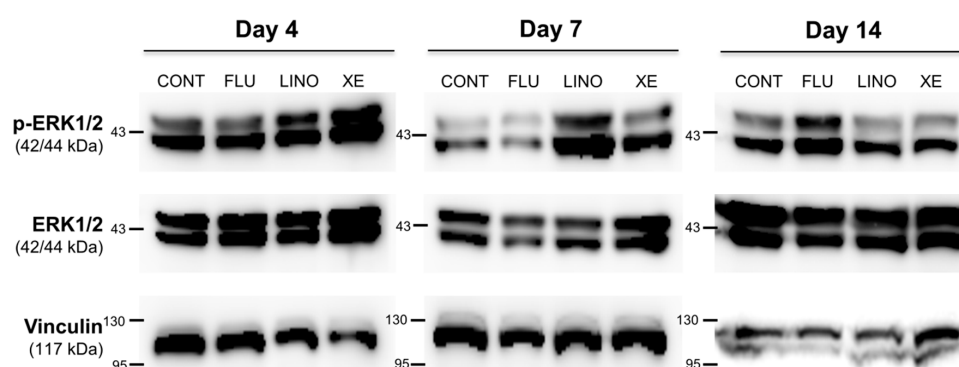


**Figure 9.** Alterations of ERK1/2 phosphorylation by the  $K_V7$  opener or  $K_V7.3$  blockers in MG-63 cells. Western blot analysis showed that, while linopirdine (30  $\mu$ M) and XE991 (10  $\mu$ M) increased the expression level of ERK1/2 phosphorylation at days 4 and 7 of osteoblast induction, flupirtine (30  $\mu$ M) had no significant effect on the level of ERK1/2 phosphorylation. Treatment with linopirdine or XE991 showed no increase of ERK1/2 phosphorylation at day 14 of osteoblast differentiation ( $n = 3$ ). Flupirtine augmented the expression of ERK1/2 phosphorylation at day 14 ( $n = 3$ ). Vinculin is used as a loading control for Western blot analysis. CONT: non-treated controls; FLU: flupirtine; LINO: linopirdine; XE: XE991; ERK1/2: extracellular-signal-regulated kinase 1/2; p-ERK: ERK1/2 phosphorylation.

### 2.7. Induction of Glutamate Release and Type 1 Collagen by $K_V7.3$ Channels during MG-63 Osteoblast Differentiation

To investigate the effect of  $K_V7$  channels on glutamate release during osteoblastic differentiation, we measured the amount of extracellular glutamate secreted by osteoblasts. Figure 9 demonstrates the difference of total glutamate amounts between the control groups and the groups treated with flupirtine (30  $\mu$ M), linopirdine (30  $\mu$ M), and XE991 (10  $\mu$ M). The  $K_V7$  activation by flupirtine significantly reduced the amount of glutamate release on days 2 and 4 after inducing osteoblast differentiation (Figure 10A,B). In contrast, the  $K_V7.3$  blockade by linopirdine or XE991 increased the amount of extracellular glutamate (Figure 10A,B).

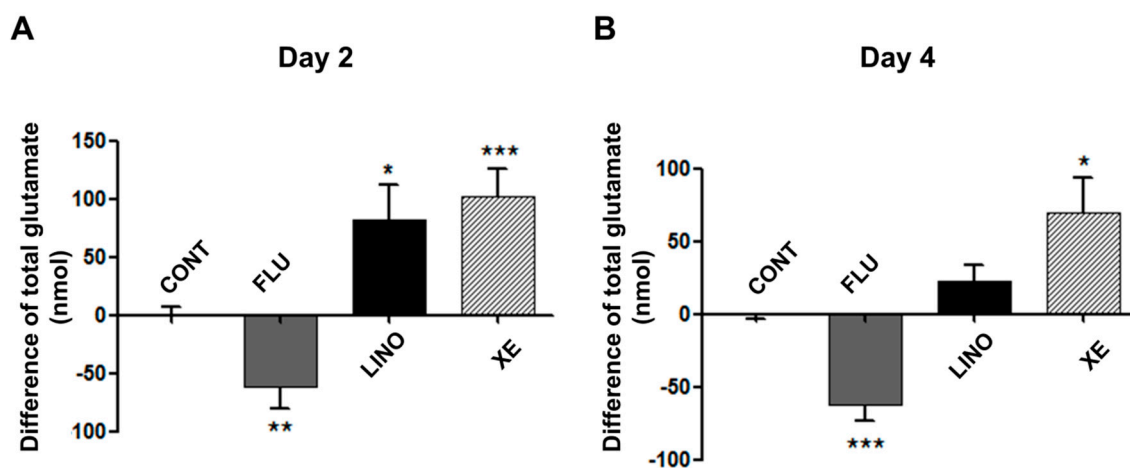


**Figure 10.** Effect of  $K_V7$  channel on glutamate release during osteoblastic differentiation in MG-63 cells. (A) On day 2, flupirtine (30  $\mu$ M) significantly decreased glutamate release after inducing osteoblastic differentiation ( $n = 6$ ). However, linopirdine (30  $\mu$ M) or XE991 (10  $\mu$ M) caused significantly increased glutamate release ( $n = 5$ ); (B) On day 4, flupirtine also caused decreased glutamate release ( $n = 5$ ), whereas XE991 notably increased the extracellular glutamate ( $n = 7$ ). Linopirdine augmented the amount of glutamate, but not statistically significantly ( $n = 8$ ). The values are presented as mean  $\pm$  SEM. \*  $p < 0.05$ ; \*\*  $p < 0.01$ ; and \*\*\*  $p < 0.005$ . CONT: non-treated controls; FLU: flupirtine; LINO: linopirdine; XE: XE991.

To examine whether the augmentation of glutamate release by  $K_V7.3$  blockers can directly promote osteoblastic differentiation, CNQX (6-cyano-7-nitroquinoxaline-2,3-dione), an AMPA  $\alpha$ -amino-3-hydroxy-5-methyl-4-isoxazolepropionic acid/kainite receptor antagonist, and MK801, an NMDA (*N*-methyl-D-aspartate) receptor antagonist, were used. Mineralized deposits augmented by  $K_V7.3$  blockers were reduced by co-application of CNQX (50  $\mu$ M) (Figure 11A,B) and MK801 (50  $\mu$ M) (Figure 12A,B). Additionally, CNQX treatment with linopirdine or XE991 attenuated the expression of ALP at days 4 and 7 (Figure 11C), whereas the OSC level was not affected (Figure 11D). Treatment with MK801 and  $K_V7.3$  blockers reduced the ALP levels at days 4 and 7 (Figure 12C), and linopirdine and flupirtine with MK801 attenuated the OSC levels at day 7 (Figure 12D). Riluzole, a glutamate release inhibitor, was also applied. Riluzole (30  $\mu$ M) co-applied with linopirdine (30  $\mu$ M) or XE991 (10  $\mu$ M) counteracted the promotive effects of linopirdine and XE991 alone on extracellular mineralization (Figure 13A,B). The mRNA expression of ALP was decreased by riluzole treatment with  $K_V7.3$  blockers, including linopirdine or XE991, at day 4 (Figure 13C), while riluzole with linopirdine or XE991 attenuated the OSC level at day 7 (Figure 13D). However, co-treatment with riluzole and the  $K_V7$  opener—flupirtine (30  $\mu$ M)—caused no significant changes in the matrix mineralization (Figure 13A,B) or in the expression of ALP and OSC (Figure 13C,D). These results suggested that glutamate receptor antagonism or glutamate release inhibition counteracted the promotive effects of linopirdine and XE991 on matrix mineralization during osteoblastic differentiation.

To further understand the role of  $K_V7.3$  channels in extracellular matrix mineralization, the expression of intracellular type 1 collagens, which are involved in matrix maturation during osteoblast differentiation, was investigated. The blockade of  $K_V7.3$  by linopirdine (30  $\mu\text{M}$ ) or XE991 (10  $\mu\text{M}$ ) augmented the level of type 1 collagens on day 7 of osteoblastic differentiation. The  $K_V7$  activation by flupirtine (30  $\mu\text{M}$ ) decreased the expression of type 1 collagens (Figure 14).

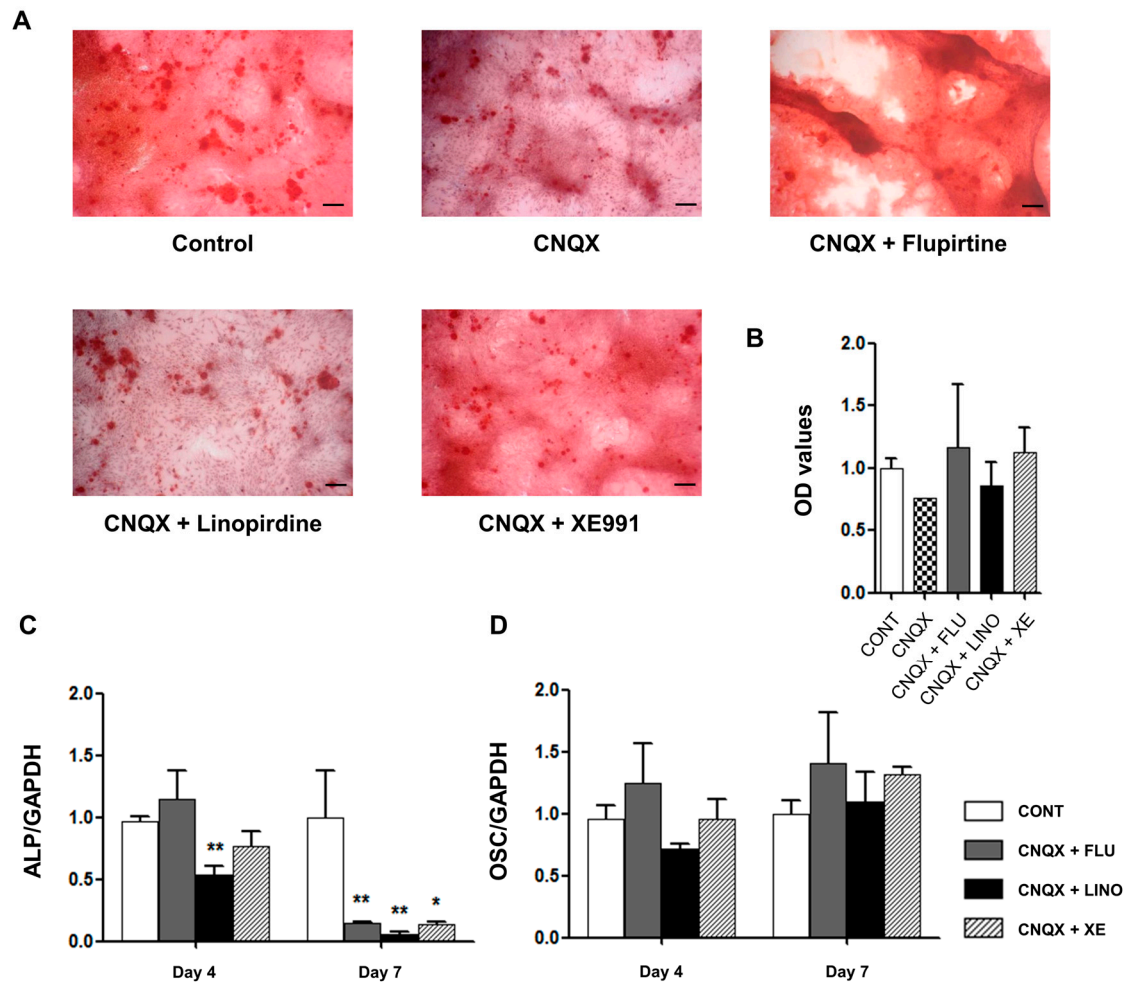


**Figure 11.** Suppressive effect of CNQX (6-cyano-7-nitroquinoxaline-2,3-dione), an AMPA ( $\alpha$ -amino-3-hydroxy-5-methyl-4-isoxazolepropionic acid)/kainite receptor antagonist, on osteoblastic differentiation promoted by  $K_V7.3$  blockers. (A) Alizarin Red S staining showed that CNQX (50  $\mu\text{M}$ ) co-applied with flupirtine (30  $\mu\text{M}$ ), linopirdine (30  $\mu\text{M}$ ), or XE991 (10  $\mu\text{M}$ ) produced amounts of calcium deposits similar to those of the controls ( $n = 3$ ). (B) The OD values are shown parallel to Alizarin Red S staining results. The relative mRNA expression levels of osteoblastic differentiation markers, including ALP and OSC, were measured with qRT-PCR and normalized against GAPDH (glyceraldehyde 3-phosphate dehydrogenase) expression ( $n = 3$ ). (C) At day 4, CNQX treatment with XE991 significantly reduced the ALP mRNA expression. At day 7, CNQX with flupirtine, linopirdine, or XE991 attenuated the ALP level. (D) CNQX treatment with flupirtine, linopirdine, or XE991 showed no significant changes in the OSC levels. Data are presented as mean  $\pm$  SEM. \*  $p < 0.05$  and \*\*  $p < 0.01$ . Scale bar represents 100  $\mu\text{m}$ . CONT: non-treated controls; FLU: flupirtine; LINO: linopirdine; XE: XE991; ALP: alkaline phosphatase; OSC: osteocalcin; OD: optical density.

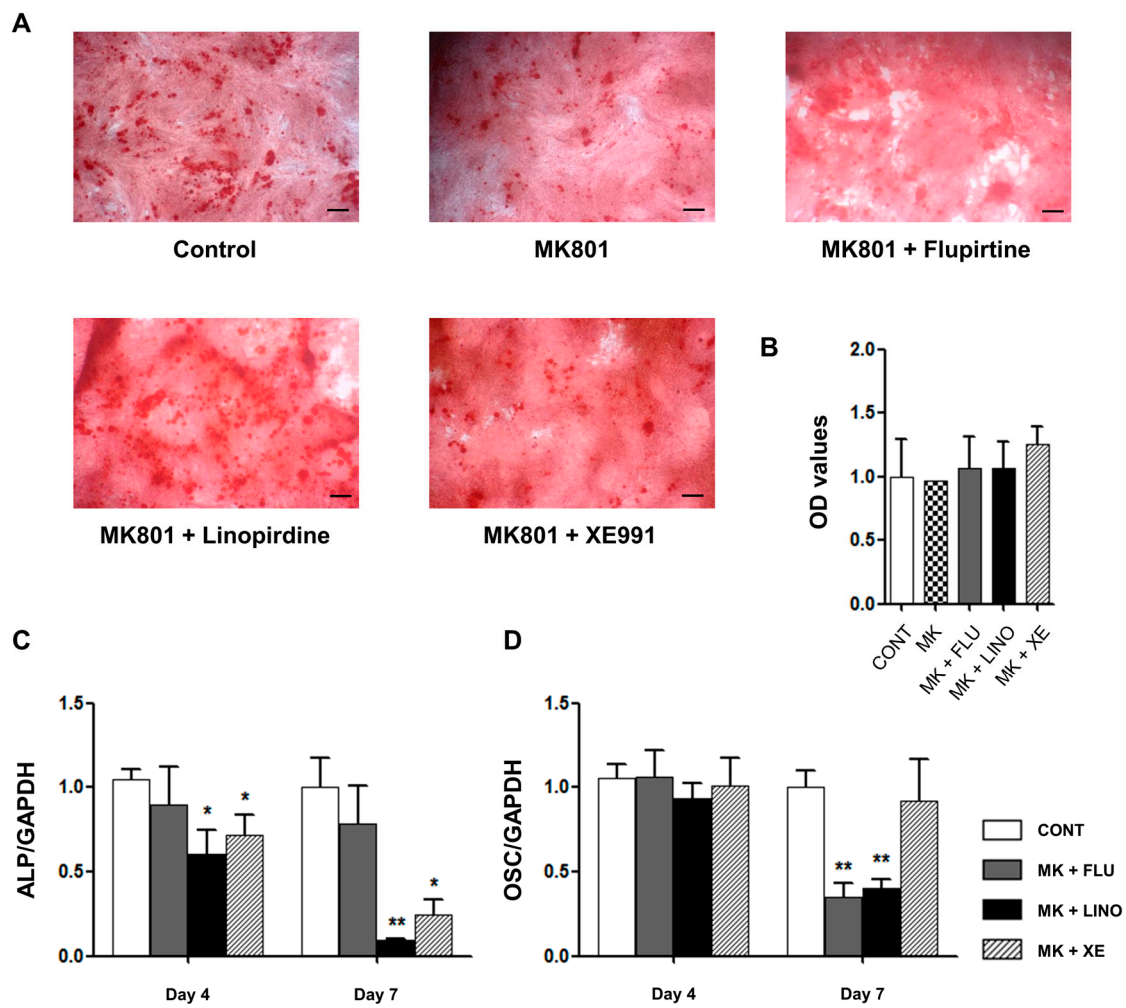


**Figure 12.** Suppressive effect of MK801, an NMDA (N-methyl-D-aspartate) receptor antagonist, on osteoblastic differentiation promoted by  $K_v7.3$  blockers. (A) Alizarin Red S staining showed that MK801 (50  $\mu$ M) treatment co-applied with flupirtine (30  $\mu$ M), linopirdine (30  $\mu$ M), or XE991 (10  $\mu$ M) produced amounts of calcium deposits similar to those of the controls ( $n = 3$ ); (B) The OD values are shown parallel to Alizarin Red S staining results. The relative mRNA expression levels of osteoblastic differentiation markers, including ALP and OSC, were measured with qRT-PCR and normalized against GAPDH (glyceraldehyde 3-phosphate dehydrogenase) expression ( $n = 3$ ); (C) At days 4 and 7, MK801 treatment with linopirdine or XE991 attenuated ALP mRNA expression; (D) At day 7, MK801 treatment with flupirtine or linopirdine significantly reduced OSC mRNA expression. Data are presented as mean  $\pm$  SEM. \*  $p < 0.05$  and \*\*  $p < 0.01$ . Scale bar represents 100  $\mu$ m. CONT: non-treated controls; MK: MK801; FLU: flupirtine; LINO: linopirdine; XE: XE991; ALP: alkaline phosphatase; OSC: osteocalcin; OD: optical density.

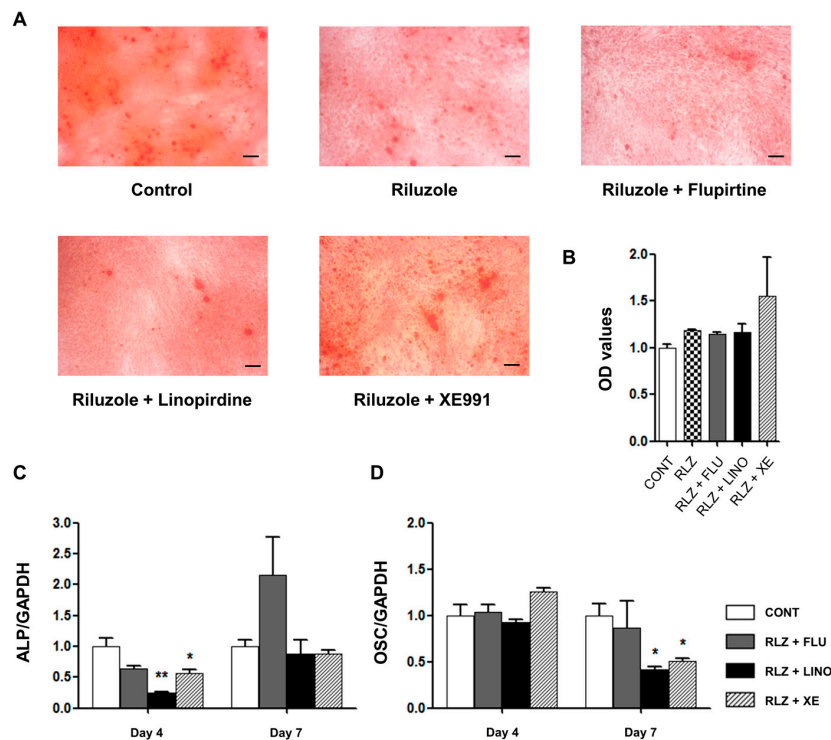


**Figure 13.** Counter-effect of riluzole, a glutamate release inhibitor, on osteoblastic differentiation promoted by  $K_V7.3$  blockers. (A) Alizarin Red S staining showed that riluzole (30  $\mu$ M) co-applied with flupirtine (30  $\mu$ M), linopirdine (30  $\mu$ M), or XE991 (10  $\mu$ M) produced mineralization levels similar to those of the controls ( $n = 3$ ); (B) The OD values are shown parallel to Alizarin Red S staining results. The relative mRNA expression levels of osteoblastic differentiation markers, including ALP and OSC, were measured with qRT-PCR and normalized against GAPDH (glyceraldehyde 3-phosphate dehydrogenase) expression ( $n = 3$ ); (C) At day 4, riluzole treatment with linopirdine or XE991 reduced the mRNA expression of ALP. At day 7, there was no significant change in ALP levels, although riluzole treatment with flupirtine had a tendency to increase these levels; (D) At day 7, riluzole treatment with linopirdine or XE991 reduced the OSC mRNA expression. Data are presented as mean  $\pm$  SEM. \*  $p < 0.05$  and \*\*  $p < 0.01$ . Scale bar represents 100  $\mu$ m. CONT: non-treated controls; RLZ: riluzole; FLU: flupirtine; LINO: linopirdine; XE: XE991; ALP: alkaline phosphatase; OSC: osteocalcin; OD: optical density.

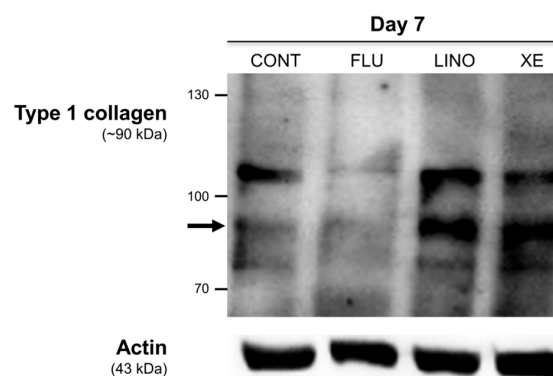


**Figure 14.** Induction of intracellular type 1 collagen by  $K_V7$  channel during osteoblast differentiation in MG-63 cells. Western blot analysis demonstrated that 30  $\mu$ M of linopirdine or 10  $\mu$ M of XE991 considerably increased the expression of type 1 collagen on day 7 of osteoblastic induction, while 30  $\mu$ M of flupirtine attenuated type 1 collagens. CONT: non-treated controls; FLU: flupirtine; LINO: linopirdine; XE: XE991.

### 3. Discussion

The present study demonstrates that  $K_V7.3$  channels have potential effects on osteoblast differentiation. Our results showed that blockade of  $K_V7.3$  channels by linopirdine or XE991 remarkably increased extracellular mineralization during osteoblast differentiation. In contrast, activation of  $K_V7.3$  channels by flupirtine did not produce significant changes. The osteoblast marker genes, ERK1/2 phosphorylation, synaptic-vesicle protein, synapsin, glutamate signals, and type 1 collagens were also involved in the process of osteoblast differentiation.

Several studies have reported that ion channels, including voltage-gated calcium channels [53] and ether-à-go-go 1 channels [54–56], are involved in cell proliferation in MG-63 or Saos-2 cells. However, ion channels are not widely known for regulating osteoblast differentiation. The overexpression of chloride channel-3 enhances osteogenic differentiation through Runx2-mediated ALP, BSP, and OSC genes by regulating intracellular pH in MC3T3-E1 primary mouse osteoblasts [57]. Chloride intracellular channel 1 also induces osteoblast marker genes by hyperpolarization of the mitochondrial membrane in C3H10T1/2 mouse embryonic mesenchymal cells [58]. Among the  $K^+$  channels, the inwardly rectifying potassium channel Kir2.1 was recently reported to regulate osteoblastic differentiation, and blockade of Kir2.1 attenuated matrix mineralization, suggesting that Kir2.1 channel is critical during osteoblastogenesis [59]. In contrast, blockade of large-conductance potassium channels with TEA increased mineralization in human primary osteoblasts [60], and hSlo potassium channels are reported to regulate bone remodeling by responding the mechanical loads in MG-63 and CAL72 osteosarcoma cells [61].

Most studies concerning osteoblast differentiation have focused on mesenchymal stem cells (MSCs) [58] or primary osteoblasts [57,60]. Our study, however, used MG-63 and Saos-2 osteoblast-like cells, which have distinct characteristics compared to MSCs or primary osteoblasts [62,63]. MG-63 is the immature state of the osteoblast, and the expressions of OSC, BSP, and Runx2 osteoblast markers are relatively lower than those of primary osteoblasts, with inconsistencies in mineralization [62,63]. Unlike MG-63, Saos-2 mature osteoblast cells have high levels of ALP enzymatic activity and a strong capability to create a calcified matrix [62], which was shown in our experiments. Another report showed dissimilar patterns of osteoblast genes, such as Runx2, in the osteoblast differentiation of Saos-2 cells in comparison to primary osteoblasts [64]. This is because MSCs can differentiate into pre-osteoblasts, immature osteoblasts, and mature osteoblasts sequentially [44], but the Saos-2 cells are the mature state of the osteoblast. Hence, Saos-2 and MG-63 cells undergo osteoblastic differentiation from the immature or mature state of osteoblasts [62], making it possible to concentrate on osteoblast maturation and matrix mineralization [65].

To date, little is known about the role of  $K_V$  channels in MG-63 and Saos-2 cells. Although several studies confirmed the existence of TEA-sensitive [66] or  $K_V2.1$ -related outward  $K_V$  currents [67], and the existence of  $K_V7$  channels has been demonstrated in MG-63 cells [23], the physiologic functions of  $K_V7$  channels in MG-63 and Saos-2 cells are not widely known. In the present study, we identified the mRNA and protein expression of  $K_V7.3$  channels in MG-63 and Saos-2 cells. Although we also demonstrated that functional  $K_V7.3$  currents were present in MG-63 cells, the  $K_V7.3$  currents were not significantly increased during osteoblastic differentiation. Recently, it has been demonstrated that several  $K_V$  channels are expressed in the intracellular region of cells, such as the nucleus [68,69] and mitochondria [70]. Therefore, we consider the possibility that intracellular  $K_V7.3$  could be involved in the differentiation process. Moreover, during osteoblast differentiation,  $K_V7.3$  mRNA expression in these cells initially declined, then increased remarkably at day 14. Similar to our results, alterations of gene expressions during differentiation have been reported in studies of ion channels [26,71,72]. Variation of the pannexin 2 gene was observed in neurogenesis [71] and  $K_V3.1$  transcript levels were shown to oscillate during adipogenesis [26]. Unlike the variation of  $K_V7.3$  transcripts, expression of  $K_V7.3$  proteins remained at the same levels, then was augmented after day 4. Although these discrepancies between mRNA and proteins are commonly seen, the reason for this is not clear. Some reports have demonstrated that mRNA and protein expression levels are relative but not causative [73], and are affected by many factors, such as mRNA stabilization, translational modification, and protein degradation [74].

Mineralization occurs within the extracellular matrix at an end-stage of osteoblast differentiation [44,47]. Hence, extracellular matrix mineralization is used as an indicator to determine osteoblast differentiation or maturation [44]. First, blockade of  $K_V$  channels by TEA augmented the mineralized deposits during osteoblast differentiation of hMSCs. Although treatment with TEA substantially decreased cell viability, the overall blockade of  $K_V$  channels promoted extracellular matrix mineralization in hMSCs. Due to the fact that  $K_V7$  channels are sensitive to TEA [36,75] and there is a relationship between the M-current of  $K_V7$  channels and  $Ca^{2+}$  [30,48–52], a key factor of bone homeostasis, we examined the effect of  $K_V7$  channels on osteoblast differentiation by conducting MG-63 and Saos-2 osteoblast-like cells. The results showed that the inhibition of  $K_V7.3$  by linopirdine and XE991 produced more mineralized deposits. On the other hand,  $K_V7$  activation by flupirtine did not increase calcium deposits in the extracellular matrix.

Bone cell differentiation involves the distinct sequential expressions of different transcription factors and bone matrix proteins at each step [44,45].  $K_V7.3$  blockade increased osterix, but did not affect Runx2, a known transcription factor that is a pivotal regulator in differentiating pluripotent stem cells into immature osteoblasts; it also induces essential osteoblast-derived matrix proteins [44]. However, the level of Runx2 expression declines with bone cell differentiation [76]. In fact, Runx2 suppresses osteoblast mineralization during bone development [65], and *in vivo* studies have demonstrated that overexpression of the Runx2 gene inhibits bone development during the maturation period [77,78]. Furthermore, Runx2 is required for the initial induction of bone matrix proteins, whereas it is not essential for maintaining them [65]. Since MG-63 cells are immature osteoblasts, the effect of the Runx2 transcription factor is not influential [62,63]. Osterix acts as a downstream signal of Runx2 and activates osteoblast marker genes, such as type 1 collagens and BSP [79,80]. ALP and OSC mRNA were also increased by suppressing  $K_V7.3$  channels. ALP and OSC are bone matrix proteins induced by the transcription factors of bone formation [81]. In this regard,  $K_V7.3$  inhibition stimulated not Runx2 but osterix, a downstream signal, to induce the levels of ALP and OSC, which promoted matrix mineralization.

Glutamate, the most common excitatory neurotransmitter, is primarily found in the central nervous system (CNS). However, glutamate signaling is not confined to the CNS; it is also found in non-neuronal tissues, including lung [82], megakaryocytes [83], pancreas [84–86], and bone [87–91]. Specifically, glutamatergic innervation exists in bones, similar to that of the CNS [89]. Glutamate is released from bone cells, in turn acting as an autologous signal within the bone environment, facilitating osteoblast proliferation, differentiation, and maturation [87,88,90–92]. Other studies have reported that treatment with glutamate receptor agonists, such as AMPA or NMDA, increased OSC levels, ALP activity, and mineralization of calcium deposits in bone matrix *in vitro* [87,90,91]. Moreover, *in vivo* studies have indicated that local injection of AMPA or NMDA into bone augments bone volume and mass [87].

MG-63 cells express the mRNA of various types of glutamate receptors, including NMDA receptors (NR)—NR1, NR2A, NR2B, NR2D, and NR3A—and some metabotropic receptors (mGluR) including mGluR1, mGluR2, mGluR3, mGluR4, mGluR5, and mGluR8 [93]. The mechanism of glutamate regulation is analogous to that of synapses in the CNS [89]. The exocytosis of glutamate is involved in the activity of synapsin via adjusting the phosphorylation of the ERK signal [94–96]. Additionally, the  $K_V7.2/7.3$  channel has been reported to be engaged in the phosphorylation of ERK1/2 in hippocampal neurons [97]. Hence, we studied whether ERK1/2 and synapsin proteins are responsible for glutamate exocytosis. The results showed that ERK1/2 phosphorylation was increased by the  $K_V7.3$  blockade on days 4 and 7, and the overall levels of synapsin by  $K_V7.3$  inhibition were higher than with  $K_V7$  activation. To further confirm that the glutamate induced by  $K_V7.3$  blockers can affect extracellular mineralization, glutamate receptor antagonists (CNQX and MK801) and a glutamate release inhibitor (riluzole) were co-applied with  $K_V7$  drugs. CNQX, MK801, and riluzole suppressed the promotive effects of  $K_V7.3$  blockers on mineralization. Hence, the blockade of  $K_V7.3$  enhanced the glutamate signals, which ultimately promoted the matrix mineralization.

Collagens are also involved in matrix mineralization during bone cell differentiation [47,98–102]. They accumulate in the extracellular matrix, promoting the formation of extracellular calcium deposits [47,98,101,102]. Mutations in collagen genes, especially type 1 collagens, is one of the

factors that cause osteogenesis imperfecta [101,103,104]. We confirmed that the level of intracellular type 1 collagens was enhanced by the blockade of  $K_V7.3$  channels, whereas  $K_V7$  activation caused no significant difference. Thus, we concluded that the increase of type 1 collagens promoted the maturation and mineralization of the bone cell matrix.

Taken together, our findings suggest that  $K_V7.3$  may have potential as a regulator of osteoblast differentiation. The results indicated that inhibition of the  $K_V7.3$  channel led to the augmentation of osterix expression, and it also increased the extracellular glutamate release that responds to the upregulation of synapsin mediated by ERK1/2 phosphorylation. These pathways resulted in increased ALP and OSC mRNA, as well as deposition of type 1 collagen proteins, which subsequently enhanced extracellular matrix mineralization during osteoblast differentiation. Osteopenia and osteoporosis are common health problems around the world [105]. Medications for osteoporosis are generally anti-resorptive reagents acting on osteoclasts [40,106–109] and the modulators of estrogen [110], calcitonin [109,111], and parathyroid hormone [40,109] to increase blood  $Ca^{2+}$  concentration. However, side effects have been reported with drugs that have inhibitory effects on osteoclasts, such as bone fractures [112,113], skeletal pain [113,114], and increased risk of cancer [115,116]. Hormone-modulating agents also have potential adverse effects [110,111]. Therefore, advanced treatment has recently been explored, such as targeting molecular pathways [40]. In this respect, although further studies are necessary to elucidate the specific mechanisms in a living body,  $K_V7.3$  channel might serve as a potential therapeutic target for bone-loss-related diseases.

## 4. Materials and Methods

### 4.1. Materials

Tetraethylammonium (TEA) a non-specific  $K_V$  channel blocker, was obtained from Sigma-Aldrich (St. Louis, MO, USA).  $K_V7$  channel modulators, including flupirtine maleate, linopirdine dihydrochloride, and XE991 dihydrochloride, were purchased from Tocris Bioscience (Minneapolis, MN, USA). Riluzole, a glutamate release inhibitor, and CNQX and MK801, glutamate receptor antagonists, were obtained from Tocris Bioscience.

Rabbit polyclonal anti- $K_V7.3$  antibody was obtained from Alomone Labs (Jerusalem, Israel). Rabbit polyclonal anti-ERK1/2 and phospho-ERK1/2 antibody were purchased from Cell Signaling Technology (Danvers, MA, USA) and goat polyclonal synapsin Ia/b and goat polyclonal type 1 collagen antibody were purchased from Santa Cruz Biotechnology, Inc. (Dallas, TX, USA). Horseradish peroxidase-conjugated anti-rabbit, anti-mouse antibodies were purchased from GenDEPOT (Barker, TX, USA) and the anti-goat antibody came from Santa Cruz Biotechnology, Inc.

### 4.2. Cell Culture and Osteoblast Induction

Cultured hMSCs, derived from the iliac crests of normal human donors, were purchased from Pharmicell Co., Ltd. (Seoul, South Korea). The hMSCs were maintained in the growth medium (GM) consisting of low-glucose Dulbecco's modified Eagle's medium (DMEM) containing 10% fetal bovine serum (FBS), 0.3 mg/mL of glutamine, 100 units/mL of penicillin, and 100  $\mu$ g/mL of streptomycin at 37 °C in a humidified atmosphere of 95% air and 5%  $CO_2$ . hMSCs at passages 4–5 were used in all experiments.

MG-63 cells and Saos-2 cells were purchased from Korean Cell Line Banks (Seoul, South Korea). MG-63 cells were cultured in GM consisting of high-glucose DMEM containing 10% FBS and 1% antibiotic antimycotic solution in an incubator at 37 °C with 95% air and 5%  $CO_2$ . Saos-2 cells were maintained in Rosewell Park Memorial Institute (RPMI) 1640 medium with 25 mM HEPES (4-(2-hydroxyethyl)-1-piperazineethanesulfonic acid) containing 10% FBS and 1% antibiotic antimycotic solution, under the same conditions. MG-63 cells at passages 121–130 and Saos-2 cells at passages 52–61 were used in all experiments.

To induce osteoblast differentiation, 50 mg/mL of ascorbic acid (Sigma-Aldrich), 10 mM of  $\beta$ -glycerophosphate (Sigma-Aldrich), and 10 nM of dexamethasone (Sigma-Aldrich) were added to the maintenance GM. For osteoblast differentiation, cells were harvested using trypsin/EDTA.

The detached cells were then plated onto 6-well plates at a density of  $10^5$  cells/well for 24 h to allow cell attachment. On the following day, the cells were pre-incubated with flupirtine (30  $\mu$ M), linopirdine (30  $\mu$ M), XE991 (10  $\mu$ M), riluzole (50  $\mu$ M), CNQX (50  $\mu$ M), and MK801 (50  $\mu$ M) for 2 h, and then transferred to an osteoblast-induction medium (OM) containing these drugs and left for 14 days. The drug-containing medium was replaced twice a week. Cells in the control groups were pre-incubated with GM for 2 h, and then transferred to OM without drugs for 14 days.

#### 4.3. Cell Viability Assay

An Alamar Blue assay was used to determine the cytotoxicity of TEA (10 mM) by adding 10X Alamar Blue solution (Biosource, Blue Bell, PA, USA) to each culture well, and the plates were incubated at 37 °C for 2 h. The absorbance of the plates was then measured at 570 nm, normalized to the OD values at 620 nm as a reference wavelength.

The MTT (3-(4,5-dimethylthiazol-2-yl)-2,5-diphenyltetrazolium bromide) assay was used to measure the cytotoxicity of flupirtine (30  $\mu$ M), linopirdine (30  $\mu$ M), and XE991 (10  $\mu$ M). The concentration of these drugs was based on the EC<sub>50</sub> or IC<sub>50</sub> value for each drug. MG-63 cells were plated onto 96-well plates at a concentration of  $10^4$  cells/well in GM or OM. The cells were treated with flupirtine, linopirdine, and XE991 for 24, 48, and 72 h, respectively. After washing the cells with Dulbecco's Phosphate-Buffered Saline (DPBS), they were incubated with 200  $\mu$ L of DPBS containing 0.5 mg/mL of MTT for 4 h. The formazans created by the viable cells were solubilized with 200  $\mu$ L of dimethylsulfoxide. The absorbance of each well was measured at 570 nm.

#### 4.4. RNA Extraction, RT-PCR and qRT-PCR

Total cellular RNA was extracted with RiboEx™ (GeneAll, Seoul, South Korea) and DNase I (TaKaRa, Nojihigashi, Japan) according to the manufacturer's protocol. To synthesize cDNA, 1  $\mu$ g of RNA was used by M-MLV reverse transcriptase (Invitrogen, Waltham, MA, USA). Specific primers were employed for RT-PCR (Table 1). The PCR products were then electrophoresed in a 1.6% agarose gel and the expression levels of the target genes were confirmed quantitatively by real-time PCR (Applied Biosystems, Waltham, MA, USA) using SYBR® Premix Ex Tag (TaKaRa). Gene expression was quantified using the comparative threshold cycles, and the relative gene expressions were compared to the ratios of the reference gene (GAPDH) threshold cycles.

**Table 1.** Sequences of PCR primers used for RT-PCR and quantitative PCR.

Gene	Primer	Sequence	Product Size (bp)	Accession Numbers
<i>K<sub>V</sub>7.1</i>	Forward	CCCAAGAAGTCTGTGGTGGT	154	NM_000218
	Reverse	TGTCATAGCCCGTCGACAGAG		
<i>K<sub>V</sub>7.2</i>	Forward	GCAAGCTGCAGAATTCCTC	201	NM_004518
	Reverse	AGTACTCCACGCCAAACACC		
<i>K<sub>V</sub>7.3</i>	Forward	GGTGCAGGTCACGGAGTATT	174	NM_001204824
	Reverse	GGGCTGACTTTGTCAATGGT		
<i>K<sub>V</sub>7.4</i>	Forward	CTGGGCATCTCTTTCTTTGC	160	AH007377
	Reverse	GTACCAGGTGGCTGTCAGGT		
<i>K<sub>V</sub>7.5</i>	Forward	CGCTTTCGTTTTTCTCCTTG	207	NM_001160134
	Reverse	CGAGCAAACCTCAGTCTTCC		
<i>ALP</i>	Forward	CCTCCTCGGAAGACACTCTG	139	NM_000478
	Reverse	GCAGTGAAGGGCTTCTTGTC		
<i>OSC</i>	Forward	GACTGTGACGAGTTGGCTGA	119	NM_001199662
	Reverse	CTGGAGAGGAGCAGAACTGG		
<i>Runx2</i>	Forward	CACCGAGACCAACAGAGTCA	95	NM_001015051
	Reverse	TGATGCCATAGTCCCTCCTT		
<i>Osterix</i>	Forward	GCCAGAAGCTGTGAAACCTC	161	AF477981
	Reverse	GCTGCAAGCTCTCCATAACC		
<i>GAPDH</i>	Forward	CTCTGCTCCTCTGTTTCGAC	112	NM_002046
	Reverse	ACGACCAAATCCGTTGACTC		

#### 4.5. Alizarin Red S Staining and Quantification

Alizarin Red S staining was used to determine the extent of calcium deposits, an indicator of mineralization. hMSCs were cultured in OM containing TEA for 16 days. MG-63 and Saos-2 cells were cultured in OM with Kv7 modulators for 14 days. They were then fixed with 70% ice-cold ethanol for 1 h and stained with 2% Alizarin Red S solution, pH 4.1–4.3 (Sigma-Aldrich). After Alizarin Red S staining, the cells were dissolved in 10% cetylpyridinium chloride, and the OD values at 570 nm were analyzed for the quantification of calcium deposits.

#### 4.6. Western Blot Analysis

Total cell lysates were extracted by treating the cells with a lysis buffer containing 50 mM of Tris-HCl (pH 8.0) with 150 mM of sodium chloride, 1.0% igeal CA-630 (NP-40), 0.5% sodium deoxycholate, and 0.1% sodium dodecyl sulfate (Sigma-Aldrich) and by adding 1% protease inhibitors (Sigma-Aldrich) and 10% phosphatase inhibitors (Roche, Basel, Switzerland). The cell lysates were incubated on ice for 10 min and centrifuged at  $10,000\times g$  for 10 min at 4 °C, and the supernatant was used for the whole-cell lysates. The bicinchoninic acid (BCA) assay was used to determine protein concentrations.

SDS-PAGE electrophoresis was conducted on 8%–12% acrylamide gels according to the size of target proteins, and the separated proteins were transferred onto the nitrocellulose membranes. Membranes were then blocked with TBST (Tris Buffered Saline, 0.1% Tween-20) containing 5% skim milk for 1 h at room temperature. Specific antibodies were added to TBST containing 5% skim milk, and the membranes were incubated at 4 °C overnight. After washing with TBST three times, the membranes were incubated with horseradish peroxidase-conjugated anti-rabbit, anti-mouse, or anti-goat antibodies for 1 h at room temperature. After washing with TBST three times, proteins were identified using enhanced chemiluminescence (ECL) solution (Advansta Inc., Adams, CA, USA).

#### 4.7. Extracellular Glutamate Assay

The release of glutamate into the culture medium by MG-63 cells was measured with a glutamate colorimetric assay kit (BioVision Inc., Milpitas, CA, USA) according to the manufacturer's procedure. To determine the release of glutamate into the extracellular medium, the cells were plated onto 6-well plates at a density of  $10^5$  cells/well, followed by the same protocol of inducing osteoblast differentiation described above. On days 2 and 4, the cultured medium was collected for glutamate assay, and the remaining cells were used for the quantification of proteins. The medium used in the glutamate assay was phenol red-free DMEM.

#### 4.8. Electrophysiological Recordings

MG-63 cells were detached using trypsin/EDTA, and then cells at density of  $5 \times 10^3$  were precipitated and suspended in the recording chamber (0.7 mL) with extracellular recording solution containing (in mM): 130 NaCl, 4 KCl, 1.8 CaCl<sub>2</sub>, 1MgCl<sub>2</sub>, 10 HEPES, and 10 glucose (adjusted to pH 7.4 with NaOH). Patch pipettes were pulled the borosilicate glass capillaries of 1.7-mm diameter and 0.5-mm wall thickness (World Precision Instruments, Sarasota, FL, USA), resulting in an open resistance ranging from 3 to 9 MΩ. The pipette internal solution (in mM) contained 110 KCl, 10 HEPES, 5 K<sub>4</sub>BAPTA, 5 K<sub>2</sub>ATP, and 1MgCl<sub>2</sub> (adjusted to pH 7.2 with KOH).

The patch electrode was located on an individual precipitated cell under bright light (BX50WI, Olympus, Tokyo, Japan) with the aid of a three-dimensional hydraulic micromanipulator (Narishige, Tokyo, Japan). Ionic currents were conducted with the whole-cell voltage-clamp configuration by using Axoclamp 2B amplifier (Axon Instruments, Foster City, CA, USA). Electric signal was filtered at 1 kHz and digitized at 10 kHz using analog-digital converter (Digidata 1320A, Axon Instruments Inc., Union City, CA, USA) and pClamp software (Version 9.0, Axon Instruments Inc.). To generate current-voltage relationships, the membrane potential was held at −80 mV, test potentials ranged from

−80 to +40 mV in 10 mV increments for 1.5 s. XE991 was applied into the external solution for blocking K<sub>V</sub>7 currents at final concentration of 50 μM.

#### 4.9. Statistical Analysis

The values were presented as mean ± standard error of the mean. Student's *t*-test was used when comparing two different groups. *p*-values of less than 0.05 were considered to be statistically significant.

### 5. Conclusions

In the present study, we identified functional K<sub>V</sub>7.3 channels in osteoblast-like cells and demonstrated its role in osteoblast differentiation. We confirmed that blockade of K<sub>V</sub>7.3 channels can promote extracellular matrix mineralization during osteoblast differentiation. The promotive effect of K<sub>V</sub>7.3 blockade on matrix mineralization was confirmed by (i) the augmentation of ALP, osteocalcin, and osterix transcripts and type 1 collagen proteins; and by (ii) the increase of extracellular glutamate release that responds to the upregulation of synapsin mediated by ERK1/2 phosphorylation. In conclusion, this study suggests that K<sub>V</sub>7.3 may be a novel regulator in osteoblast differentiation. Though further studies are required to elucidate the underlying mechanisms, our findings provide that K<sub>V</sub>7 channel may be one of the potential therapeutic targets in bone loss-related diseases.

**Acknowledgments:** This research was supported by the Basic Science Research Program through National Research Foundation of Korea (NRF) funded by the Ministry of Science, ICT & Future Planning (NRF-2012R1A2A2A01047151, NRF-2014R1A1A3A04052757).

**Author Contributions:** Ji Eun Yang performed the experiments, analyzed the data, and wrote the paper; Min Seok Song performed the experiments of hMSCs; Yiming Shen helped to perform and analyze the electrophysiological data; Pan Dong Ryu contributed reagents, materials and analyzed the data; So Yeong Lee designed the research, interpreted the data and drafted the article.

**Conflicts of Interest:** The authors declare no conflict of interest.

### References

1. Misonou, H.; Mohapatra, D.P.; Trimmer, J.S. Kv2.1: A voltage-gated K<sup>+</sup> channel critical to dynamic control of neuronal excitability. *Neurotoxicology* **2005**, *26*, 743–752. [[CrossRef](#)] [[PubMed](#)]
2. Coleman, S.K.; Newcombe, J.; Pryke, J.; Dolly, J.O. Subunit composition of Kv1 channels in human CNS. *J. Neurochem.* **1999**, *73*, 849–858. [[CrossRef](#)] [[PubMed](#)]
3. Nashmi, R.; Fehlings, M.G. Mechanisms of axonal dysfunction after spinal cord injury: With an emphasis on the role of voltage-gated potassium channels. *Brain Res. Brain Res. Rev.* **2001**, *38*, 165–191. [[CrossRef](#)]
4. Bijlenga, P.; Occhiodoro, T.; Liu, J.H.; Bader, C.R.; Bernheim, L.; Fischer-Lougheed, J. An ether-a-go-go K<sup>+</sup> current, Ih-eag, contributes to the hyperpolarization of human fusion-competent myoblasts. *J. Physiol.* **1998**, *512*, 317–323. [[CrossRef](#)] [[PubMed](#)]
5. Hancox, J.C.; McPate, M.J.; El Harchi, A.; Zhang, Y.H. The hERG potassium channel and hERG screening for drug-induced torsades de pointes. *Pharmacol. Ther.* **2008**, *119*, 118–132. [[CrossRef](#)] [[PubMed](#)]
6. Grunnet, M.; Hansen, R.S.; Olesen, S.P. Herg1 channel activators: A new anti-arrhythmic principle. *Prog. Biophys. Mol. Biol.* **2008**, *98*, 347–362. [[CrossRef](#)] [[PubMed](#)]
7. Martire, M.; Castaldo, P.; D'Amico, M.; Preziosi, P.; Annunziato, L.; Tagliatela, M. M channels containing KCNQ2 subunits modulate norepinephrine, aspartate, and gaba release from hippocampal nerve terminals. *J. Neurosci.* **2004**, *24*, 592–597. [[CrossRef](#)] [[PubMed](#)]
8. Martire, M.; D'Amico, M.; Panza, E.; Miceli, F.; Viggiano, D.; Lavergata, F.; Iannotti, F.A.; Barrese, V.; Preziosi, P.; Annunziato, L.; *et al.* Involvement of KCNQ2 subunits in [<sup>3</sup>H] dopamine release triggered by depolarization and pre-synaptic muscarinic receptor activation from rat striatal synaptosomes. *J. Neurochem.* **2007**, *102*, 179–193. [[CrossRef](#)] [[PubMed](#)]
9. Pillozzi, S.; Brizzi, M.F.; Balzi, M.; Crociani, O.; Cherubini, A.; Guasti, L.; Bartolozzi, B.; Becchetti, A.; Wanke, E.; Bernabei, P.A.; *et al.* Herg potassium channels are constitutively expressed in primary human acute myeloid leukemias and regulate cell proliferation of normal and leukemic hemopoietic progenitors. *Leukemia* **2002**, *16*, 1791–1798. [[CrossRef](#)] [[PubMed](#)]

10. Abdul, M.; Santo, A.; Hoosein, N. Activity of potassium channel-blockers in breast cancer. *Anticancer Res.* **2003**, *23*, 3347–3352. [[PubMed](#)]
11. Jang, S.H.; Kang, K.S.; Ryu, P.D.; Lee, S.Y. Kv1.3 voltage-gated K<sup>+</sup> channel subunit as a potential diagnostic marker and therapeutic target for breast cancer. *BMB Rep.* **2009**, *42*, 535–539. [[CrossRef](#)] [[PubMed](#)]
12. Ouadid-Ahidouch, H.; Chaussade, F.; Roudbaraki, M.; Slomianny, C.; Dewailly, E.; Delcourt, P.; Prevarskaya, N. Kv1.1 K<sup>+</sup> channels identification in human breast carcinoma cells: Involvement in cell proliferation. *Biochem. Biophys. Res. Commun.* **2000**, *278*, 272–277. [[CrossRef](#)] [[PubMed](#)]
13. Roy, J.; Vantol, B.; Cowley, E.; Blay, J.; Linsdell, P. Pharmacological separation of heag and hERG K<sup>+</sup> channel function in the human mammary carcinoma cell line MCF-7. *Oncol. Rep.* **2008**, *19*, 1511–1516. [[PubMed](#)]
14. Spitzner, M.; Ousingsawat, J.; Scheidt, K.; Kunzelmann, K.; Schreiber, R. Voltage-gated K<sup>+</sup> channels support proliferation of colonic carcinoma cells. *FASEB J.* **2007**, *21*, 35–44. [[CrossRef](#)] [[PubMed](#)]
15. Jiraporn, O.; Melanie, S.; Supaporn, P.; Luigi, T.; Luigi, T.; Lukas, B.; Karl, K.; Rainer, S. Expression of voltage-gated potassium channels in human and mouse colonic carcinoma. *Clin. Cancer Res.* **2007**, *13*, 824–831.
16. Lastraioli, E.; Guasti, L.; Crociani, O.; Polvani, S.; Hofmann, G.; Witchel, H.; Bencini, L.; Calistri, M.; Messerini, L.; Scatizzi, M.; *et al.* Herg1 gene and hERG1 protein are overexpressed in colorectal cancers and regulate cell invasion of tumor cells. *Cancer Res.* **2004**, *64*, 606–611. [[CrossRef](#)] [[PubMed](#)]
17. Shimizu, T.; Fujii, T.; Takahashi, Y.; Takahashi, Y.; Suzuki, T.; Ukai, M.; Tauchi, K.; Horikawa, N.; Tsukada, K.; Sakai, H. Up-regulation of Kv7.1 channels in thromboxane A<sub>2</sub>-induced colonic cancer cell proliferation. *Pflug. Arch. Eur. J. Physiol.* **2014**, *466*, 541–548. [[CrossRef](#)] [[PubMed](#)]
18. Mei, L.; Yongquan, S.; Zheyi, H.; Zhiming, H.; Yanglin, P.; Na, L.; Changcun, G.; Liu, H.; Jun, W.; Taidong, Q.; *et al.* Expression of delayed rectifier potassium channels and their possible roles in proliferation of human gastric cancer cells. *Cancer Biol. Ther.* **2005**, *4*, 1342–1347.
19. Conforti, L.; Petrovic, M.; Mohammad, D.; Lee, S.; Ma, Q.; Barone, S.; Filipovich, A.H. Hypoxia regulates expression and activity of Kv1.3 channels in T lymphocytes: A possible role in T cell proliferation. *J. Immunol.* **2003**, *170*, 695–702. [[CrossRef](#)] [[PubMed](#)]
20. Wulff, H.; Calabresi, P.A.; Allie, R.; Yun, S.; Pennington, M.; Beeton, C.; Chandy, K.G. The voltage-gated Kv1.3 K<sup>+</sup> channel in effector memory T cells as new target for ms. *J. Clin. Investig.* **2003**, *111*, 1703–1713. [[CrossRef](#)] [[PubMed](#)]
21. Jang, S.H.; Choi, S.Y.; Ryu, P.D.; Lee, S.Y. Anti-proliferative effect of Kv1.3 blockers in A549 human lung adenocarcinoma *in vitro* and *in vivo*. *Eur. J. Pharmacol.* **2011**, *651*, 26–32. [[CrossRef](#)] [[PubMed](#)]
22. Iannotti, F.A.; Panza, E.; Barrese, V.; Viggiano, D.; Soldovieri, M.V.; Tagliatela, M. Expression, localization, and pharmacological role of Kv7 potassium channels in skeletal muscle proliferation, differentiation, and survival after myotoxic insults. *J. Pharmacol. Exp. Ther.* **2010**, *332*, 811–820. [[CrossRef](#)] [[PubMed](#)]
23. Lee, B.H.; Ryu, P.D.; Lee, S.Y. Serum starvation-induced voltage-gated potassium channel Kv7.5 expression and its regulation by Sp1 in canine osteosarcoma cells. *Int. J. Mol. Sci.* **2014**, *15*, 977–993. [[CrossRef](#)] [[PubMed](#)]
24. Cherubini, A.; Hofmann, G.; Pillozzi, S.; Guasti, L.; Crociani, O.; Cilia, E.; Di Stefano, P.; Degani, S.; Balzi, M.; Olivotto, M.; *et al.* Human ether-a-go-go-related gene 1 channels are physically linked to  $\beta$ 1 integrins and modulate adhesion-dependent signaling. *Mol. Biol. Cell* **2005**, *16*, 2972–2983. [[CrossRef](#)] [[PubMed](#)]
25. Levite, M.; Cahalon, L.; Peretz, A.; Hershkoviz, R.; Sobko, A.; Ariel, A.; Desai, R.; Attali, B.; Lider, O. Extracellular K<sup>+</sup> and opening of voltage-gated potassium channels activate T cell integrin function: Physical and functional association between Kv1.3 channels and  $\beta$ 1 integrins. *J. Exp. Med.* **2000**, *191*, 1167–1176. [[CrossRef](#)] [[PubMed](#)]
26. You, M.H.; Song, M.S.; Lee, S.K.; Ryu, P.D.; Lee, S.Y.; Kim, D.Y. Voltage-gated K<sup>+</sup> channels in adipogenic differentiation of bone marrow-derived human mesenchymal stem cells. *Acta Pharmacol. Sin.* **2013**, *34*, 129–136. [[CrossRef](#)] [[PubMed](#)]
27. Zhou, X.; Song, M.; Chen, D.; Wei, L.; Yu, S.P. Potential role of KCNQ/M-channels in regulating neuronal differentiation in mouse hippocampal and embryonic stem cell-derived neuronal cultures. *Exp. Neurol.* **2011**, *229*, 471–483. [[CrossRef](#)] [[PubMed](#)]
28. Jespersen, T.; Grunnet, M.; Olesen, S.P. The KCNQ1 potassium channel: From gene to physiological function. *Physiology* **2005**, *20*, 408–416. [[CrossRef](#)] [[PubMed](#)]

29. Leung, Y.M.; Huang, C.F.; Chao, C.C.; Lu, D.Y.; Kuo, C.S.; Cheng, T.H.; Chang, L.Y.; Chou, C.H. Voltage-gated K<sup>+</sup> channels play a role in camp-stimulated neurogenesis in mouse neuroblastoma N2A cells. *J. Cell. Physiol.* **2011**, *226*, 1090–1098. [[CrossRef](#)] [[PubMed](#)]
30. Soldovieri, M.V.; Miceli, F.; Tagliatalata, M. Driving with no brakes: Molecular pathophysiology of Kv7 potassium channels. *Physiology* **2011**, *26*, 365–376. [[CrossRef](#)] [[PubMed](#)]
31. Wang, W.; Flores, M.C.; Sihm, C.R.; Kim, H.J.; Zhang, Y.; Doyle, K.J.; Chiamvimonvat, N.; Zhang, X.D.; Yamoah, E.N. Identification of a key residue in Kv7.1 potassium channel essential for sensing external potassium ions. *J. Gen. Physiol.* **2015**, *145*, 201–212. [[CrossRef](#)] [[PubMed](#)]
32. Evans, A.M.; Osipenko, O.N.; Gurney, A.M. Properties of a novel K<sup>+</sup> current that is active at resting potential in rabbit pulmonary artery smooth muscle cells. *J. Physiol.* **1996**, *496*, 407–420. [[CrossRef](#)] [[PubMed](#)]
33. Heitzmann, D.; Warth, R. No potassium, no acid: K<sup>+</sup> channels and gastric acid secretion. *Physiology* **2007**, *22*, 335–341. [[CrossRef](#)] [[PubMed](#)]
34. Pan, Z.; Kao, T.; Horvath, Z.; Lemos, J.; Sul, J.Y.; Cranstoun, S.D.; Bennett, V.; Scherer, S.S.; Cooper, E.C. A common ankyrin-G-based mechanism retains KCNQ and Nav channels at electrically active domains of the axon. *J. Neurosci.* **2006**, *26*, 2599–2613. [[CrossRef](#)] [[PubMed](#)]
35. Miceli, F.; Soldovieri, M.V.; Ambrosino, P.; Barrese, V.; Migliore, M.; Cilio, M.R.; Tagliatalata, M. Genotype-phenotype correlations in neonatal epilepsies caused by mutations in the voltage sensor of Kv7.2 potassium channel subunits. *Proc. Natl. Acad. Sci. USA* **2013**, *110*, 4386–4391. [[CrossRef](#)] [[PubMed](#)]
36. Robbins, J. KCNQ potassium channels: Physiology, pathophysiology, and pharmacology. *Pharmacol. Ther.* **2001**, *90*, 1–19. [[CrossRef](#)]
37. Iannotti, F.A.; Barrese, V.; Formisano, L.; Miceli, F.; Tagliatalata, M. Specification of skeletal muscle differentiation by repressor element-1 silencing transcription factor REST-regulated Kv7.4 potassium channels. *Mol. Biol. Cell* **2013**, *24*, 274–284. [[CrossRef](#)] [[PubMed](#)]
38. Schroeder, B.C.; Hechenberger, M.; Weinreich, F.; Kubisch, C.; Jentsch, T.J. KCNQ5, a novel potassium channel broadly expressed in brain, mediates M-type currents. *J. Biol. Chem.* **2000**, *275*, 24089–24095. [[CrossRef](#)] [[PubMed](#)]
39. Long, F. Building strong bones: Molecular regulation of the osteoblast lineage. *Nat. Rev. Mol. Cell Biol.* **2012**, *13*, 27–38. [[CrossRef](#)] [[PubMed](#)]
40. Iniguez-Ariza, N.M.; Clarke, B.L. Bone biology, signaling pathways, and therapeutic targets for osteoporosis. *Maturitas* **2015**, *82*, 245–255. [[CrossRef](#)] [[PubMed](#)]
41. Chen, G.; Deng, C.; Li, Y.P. TGF- $\beta$  and BMP signaling in osteoblast differentiation and bone formation. *Int. J. Biol. Sci.* **2012**, *8*, 272–288. [[CrossRef](#)] [[PubMed](#)]
42. Matsubara, T.; Kida, K.; Yamaguchi, A.; Hata, K.; Ichida, F.; Meguro, H.; Aburatani, H.; Nishimura, R.; Yoneda, T. BMP2 regulates osterix through Msx2 and Runx2 during osteoblast differentiation. *J. Biol. Chem.* **2008**, *283*, 29119–29125. [[CrossRef](#)] [[PubMed](#)]
43. Rahman, M.S.; Akhtar, N.; Jamil, H.M.; Banik, R.S.; Asaduzzaman, S.M. TGF- $\beta$ /BMP signaling and other molecular events: Regulation of osteoblastogenesis and bone formation. *Bone Res.* **2015**, *3*. [[CrossRef](#)] [[PubMed](#)]
44. Stein, G.S.; Lian, J.B.; van Wijnen, A.J.; Stein, J.L.; Montecino, M.; Javed, A.; Zaidi, S.K.; Young, D.W.; Choi, J.Y.; Pockwinse, S.M. Runx2 control of organization, assembly and activity of the regulatory machinery for skeletal gene expression. *Oncogene* **2004**, *23*, 4315–4329. [[CrossRef](#)] [[PubMed](#)]
45. Komori, T. Regulation of osteoblast differentiation by transcription factors. *J. Cell. Biochem.* **2006**, *99*, 1233–1239. [[CrossRef](#)] [[PubMed](#)]
46. Golub, E.E.; Boesze-Battaglia, K. The role of alkaline phosphatase in mineralization. *Curr. Opin. Orthop.* **2007**, *18*, 444–448. [[CrossRef](#)]
47. Rohde, M.; Mayer, H. Exocytotic process as a novel model for mineralization by osteoblasts *in vitro* and *in vivo* determined by electron microscopic analysis. *Calcif. Tissue Int.* **2007**, *80*, 323–336. [[CrossRef](#)] [[PubMed](#)]
48. Marrion, N.V. Control of M-current. *Annu. Rev. Physiol.* **1997**, *59*, 483–504. [[CrossRef](#)] [[PubMed](#)]
49. Marrion, N.V.; Zucker, R.S.; Marsh, S.J.; Adams, P.R. Modulation of M-current by intracellular Ca<sup>2+</sup>. *Neuron* **1991**, *6*, 533–545. [[CrossRef](#)]
50. Kosenko, A.; Hoshi, N. A change in configuration of the calmodulin-KCNQ channel complex underlies Ca<sup>2+</sup>-dependent modulation of KCNQ channel activity. *PLoS ONE* **2013**, *8*, e82290. [[CrossRef](#)] [[PubMed](#)]

51. Haitin, Y.; Attali, B. The C-terminus of Kv7 channels: A multifunctional module. *J. Physiol.* **2008**, *586*, 1803–1810. [[CrossRef](#)] [[PubMed](#)]
52. Hernandez, C.C.; Zaika, O.; Tolstykh, G.P.; Shapiro, M.S. Regulation of neural KCNQ channels: Signalling pathways, structural motifs and functional implications. *J. Physiol.* **2008**, *586*, 1811–1821. [[CrossRef](#)] [[PubMed](#)]
53. Barry, E.L. Expression of mRNAs for the  $\alpha 1$  subunit of voltage-gated calcium channels in human osteoblast-like cell lines and in normal human osteoblasts. *Calcif. Tissue Int.* **2000**, *66*, 145–150. [[CrossRef](#)] [[PubMed](#)]
54. Wu, X.; Zhong, D.; Lin, B.; Zhai, W.; Ding, Z.; Wu, J. p38 MAPK regulates the expression of ether-a-go-go potassium channel in human osteosarcoma cells. *Radiol. Oncol.* **2013**, *47*, 42–49. [[CrossRef](#)] [[PubMed](#)]
55. Wu, X.; Zhong, D.; Gao, Q.; Zhai, W.; Ding, Z.; Wu, J. MicroRNA-34a inhibits human osteosarcoma proliferation by downregulating ether-a-go-go 1 expression. *Int. J. Med. Sci.* **2013**, *10*, 676–682. [[CrossRef](#)] [[PubMed](#)]
56. Wu, J.; Zhong, D.; Fu, X.; Liu, Q.; Kang, L.; Ding, Z. Silencing of ether-a-go-go 1 by shRNA inhibits osteosarcoma growth and cell cycle progression. *Int. J. Mol. Sci.* **2014**, *15*, 5570–5581. [[CrossRef](#)] [[PubMed](#)]
57. Wang, H.; Mao, Y.; Zhang, B.; Wang, T.; Li, F.; Fu, S.; Xue, Y.; Yang, T.; Wen, X.; Ding, Y.; *et al.* Chloride channel ClC-3 promotion of osteogenic differentiation through Runx2. *J. Cell. Biochem.* **2010**, *111*, 49–58. [[CrossRef](#)] [[PubMed](#)]
58. Yang, J.Y.; Jung, J.Y.; Cho, S.W.; Choi, H.J.; Kim, S.W.; Kim, S.Y.; Kim, H.J.; Jang, C.H.; Lee, M.G.; Han, J.; *et al.* Chloride intracellular channel 1 regulates osteoblast differentiation. *Bone* **2009**, *45*, 1175–1185. [[CrossRef](#)] [[PubMed](#)]
59. Sacco, S.; Giuliano, S.; Sacconi, S.; Desnuelle, C.; Barhanin, J.; Amri, E.Z.; Bendahhou, S. The inward rectifier potassium channel Kir2.1 is required for osteoblastogenesis. *Hum. Mol. Genet.* **2015**, *24*, 471–479. [[CrossRef](#)] [[PubMed](#)]
60. Henney, N.C.; Bo, L.; Elford, C.; Reviriego, P.; Campbell, A.K.; Wann, K.T.; Evans, B.A.J. A large-conductance BK potassium channel subtype affects both growth and mineralization of human osteoblasts. *Am. J. Physiol. Cell. Physiol.* **2009**, *297*, C1397–C1408. [[CrossRef](#)] [[PubMed](#)]
61. Rezzonico, R.; Cayatte, C.; Bourget-Ponzio, I.; Romey, G.; Belhacene, N.; Loubat, A.; Rocchi, S.; van Obberghen, E.; Girault, J.A.; Rossi, B.; *et al.* Focal adhesion kinase pp125FAK interacts with the large conductance calcium-activated hSlo potassium channel in human osteoblasts: Potential role in mechanotransduction. *J. Bone Miner. Res.* **2003**, *18*, 1863–1871. [[CrossRef](#)] [[PubMed](#)]
62. Czekanska, E.M.; Stoddart, M.J.; Richards, R.G.; Hayes, J.S. In search of an osteoblast cell model for *in vitro* research. *Eur. Cell Mater.* **2012**, *24*, 1–17. [[PubMed](#)]
63. Pautke, C.; Schieker, M.; Tischer, T.; Kolk, A.; Neth, P.; Mutschler, W.; Milz, S. Characterization of osteosarcoma cell lines MG-63, Saos-2 and U-2 OS in comparison to human osteoblasts. *Anticancer Res.* **2004**, *24*, 3743–3748. [[PubMed](#)]
64. Prideaux, M.; Wijenayaka, A.R.; Kumarasinghe, D.D.; Ormsby, R.T.; Evdokiou, A.; Findlay, D.M.; Atkins, G.J. Saos2 osteosarcoma cells as an *in vitro* model for studying the transition of human osteoblasts to osteocytes. *Calcif. Tissue Int.* **2014**, *95*, 183–193. [[CrossRef](#)] [[PubMed](#)]
65. Komori, T. Regulation of osteoblast differentiation by Runx2. *Adv. Exp. Med. Biol.* **2010**, *658*, 43–49. [[PubMed](#)]
66. Yellowley, C.E.; Hancox, J.C.; Skerry, T.M.; Levi, A.J. Whole-cell membrane currents from human osteoblast-like cells. *Calcif. Tissue Int.* **1998**, *62*, 122–132. [[CrossRef](#)] [[PubMed](#)]
67. Li, X.; Zheng, S.; Dong, X.; Xiao, J. 17 $\beta$ -estradiol inhibits outward voltage-gated K<sup>+</sup> currents in human osteoblast-like MG63 cells. *J. Membr. Biol.* **2013**, *246*, 39–45. [[CrossRef](#)] [[PubMed](#)]
68. Chen, Y.; Sanchez, A.; Rubio, M.E.; Kohl, T.; Pardo, L.A.; Stuhmer, W. Functional Kv10.1 channels localize to the inner nuclear membrane. *PLoS ONE* **2011**, *6*, e19257. [[CrossRef](#)] [[PubMed](#)]
69. Jang, S.H.; Byun, J.K.; Jeon, W.I.; Choi, S.Y.; Park, J.; Lee, B.H.; Yang, J.E.; Park, J.B.; O'Grady, S.M.; Kim, D.Y.; *et al.* Nuclear localization and functional characteristics of voltage-gated potassium channel Kv1.3. *J. Biol. Chem.* **2015**, *290*, 12547–12557. [[CrossRef](#)] [[PubMed](#)]
70. Szabo, I.; Bock, J.; Grassme, H.; Soddemann, M.; Wilker, B.; Lang, F.; Zoratti, M.; Gulbins, E. Mitochondrial potassium channel Kv1.3 mediates Bax-induced apoptosis in lymphocytes. *Proc. Natl. Acad. Sci. USA* **2008**, *105*, 14861–14866. [[CrossRef](#)] [[PubMed](#)]

71. Swayne, L.A.; Wicki-Stordeur, L. Ion channels in postnatal neurogenesis: Potential targets for brain repair. *Channels* **2012**, *6*, 69–74. [[CrossRef](#)] [[PubMed](#)]
72. Yamashita, T.; Sekiguchi, A.; Iwasaki, Y.K.; Sagara, K.; Iinuma, H.; Hatano, S.; Fu, L.T.; Watanabe, H. Circadian variation of cardiac K<sup>+</sup> channel gene expression. *Circulation* **2003**, *107*, 1917–1922. [[CrossRef](#)] [[PubMed](#)]
73. Greenbaum, D.; Colangelo, C.; Williams, K.; Gerstein, M. Comparing protein abundance and mRNA expression levels on a genomic scale. *Genome Biol.* **2003**, *4*, 117–124. [[CrossRef](#)] [[PubMed](#)]
74. Vogel, C.; Marcotte, E.M. Insights into the regulation of protein abundance from proteomic and transcriptomic analyses. *Nat. Rev. Genet.* **2012**, *13*, 227–232. [[CrossRef](#)] [[PubMed](#)]
75. Hadley, J.K.; Noda, M.; Selyanko, A.A.; Wood, I.C.; Abogadie, F.C.; Brown, D.A. Differential tetraethylammonium sensitivity of KCNQ1-4 potassium channels. *Br. J. Pharmacol.* **2000**, *129*, 413–415. [[CrossRef](#)] [[PubMed](#)]
76. Maruyama, Z.; Yoshida, C.A.; Furuichi, T.; Amizuka, N.; Ito, M.; Fukuyama, R.; Miyazaki, T.; Kitaura, H.; Nakamura, K.; Fujita, T.; *et al.* Runx2 determines bone maturity and turnover rate in postnatal bone development and is involved in bone loss in estrogen deficiency. *Dev. Dyn.* **2007**, *236*, 1876–1890. [[CrossRef](#)] [[PubMed](#)]
77. Liu, W.; Toyosawa, S.; Furuichi, T.; Kanatani, N.; Yoshida, C.; Liu, Y.; Himeno, M.; Narai, S.; Yamaguchi, A.; Komori, T. Overexpression of Cbfa1 in osteoblasts inhibits osteoblast maturation and causes osteopenia with multiple fractures. *J. Cell Biol.* **2001**, *155*, 157–166. [[CrossRef](#)] [[PubMed](#)]
78. Kanatani, N.; Fujita, T.; Fukuyama, R.; Liu, W.; Yoshida, C.A.; Moriishi, T.; Yamana, K.; Miyazaki, T.; Toyosawa, S.; Komori, T. Cbfa1 regulates Runx2 function isoform-dependently in postnatal bone development. *Dev. Biol.* **2006**, *296*, 48–61. [[CrossRef](#)] [[PubMed](#)]
79. Nakashima, K.; Zhou, X.; Kunkel, G.; Zhang, Z.; Deng, J.M.; Behringer, R.R.; de Crombrugge, B. The novel zinc finger-containing transcription factor Osterix is required for osteoblast differentiation and bone formation. *Cell* **2002**, *108*, 17–29. [[CrossRef](#)]
80. Zhou, X.; Zhang, Z.; Feng, J.Q.; Dusevich, V.M.; Sinha, K.; Zhang, H.; Darnay, B.G.; de Crombrugge, B. Multiple functions of osterix are required for bone growth and homeostasis in postnatal mice. *Proc. Natl. Acad. Sci. USA* **2010**, *107*, 12919–12924. [[CrossRef](#)] [[PubMed](#)]
81. Stein, G.S.; Lian, J.B.; Owen, T.A. Relationship of cell growth to the regulation of tissue-specific gene expression during osteoblast differentiation. *FASEB J.* **1990**, *4*, 3111–3123. [[PubMed](#)]
82. Said, S.I.; Berisha, H.I.; Pakbaz, H. Excitotoxicity in the lung: N-methyl-D-aspartate-induced, nitric oxide-dependent, pulmonary edema is attenuated by vasoactive intestinal peptide and by inhibitors of poly(ADP-ribose) polymerase. *Proc. Natl. Acad. Sci. USA* **1996**, *14*, 4688–4692. [[CrossRef](#)]
83. Genever, P.G.; Wilkinson, D.J.; Patton, A.J.; Peet, N.M.; Hong, Y.; Mathur, A.; Erusalimsky, J.D.; Skerry, T. Expression of a functional N-methyl-D-aspartate-type glutamate receptor by bone marrow megakaryocytes. *Blood* **1999**, *93*, 2876–2883. [[PubMed](#)]
84. Inagaki, N.; Kuromi, H.; Gono, T.; Okamoto, Y.; Ishida, H.; Seino, Y.; Kaneko, T.; Iwanaga, T.; Seino, S. Expression and role of ionotropic glutamate receptors in pancreatic islet cells. *FASEB J.* **1995**, *9*, 686–691. [[PubMed](#)]
85. Weaver, C.D.; Yao, T.L.; Powers, A.C.; Verdoorn, T.A. Differential expression of glutamate receptor subtypes in rat pancreatic islets. *J. Biol. Chem.* **1996**, *271*, 2977–2984.
86. Molnár, E.; Váradi, A.; McIlhinney, R.A.; Ashcroft, S.J. Identification of functional ionotropic glutamate receptor proteins in pancreatic  $\beta$ -cells and in islets of langerhans. *FEBS Lett.* **1995**, *371*, 253–257. [[PubMed](#)]
87. Lin, T.H.; Yang, R.S.; Tang, C.H.; Wu, M.Y.; Fu, W.M. Regulation of the maturation of osteoblasts and osteoclastogenesis by glutamate. *Eur. J. Pharmacol.* **2008**, *589*, 37–44. [[CrossRef](#)] [[PubMed](#)]
88. Seidlitz, E.P.; Sharma, M.K.; Singh, G. Extracellular glutamate alters mature osteoclast and osteoblast functions. *Cad. J. Physiol. Pharmacol.* **2010**, *88*, 929–936. [[CrossRef](#)] [[PubMed](#)]
89. Chenu, C. Glutamatergic innervation in bone. *Microsc. Res. Tech.* **2002**, *58*, 70–76. [[CrossRef](#)] [[PubMed](#)]
90. Brakspear, K.S.; Mason, D.J. Glutamate signaling in bone. *Front. Endocrinol.* **2012**, *3*, 89–96. [[CrossRef](#)] [[PubMed](#)]
91. Genever, P.G.; Skerry, T.M. Regulation of spontaneous glutamate release activity in osteoblastic cells and its role in differentiation and survival: Evidence for intrinsic glutamatergic signaling in bone. *FASEB J.* **2001**, *15*, 1586–1588. [[CrossRef](#)] [[PubMed](#)]

92. Cowan, R.W.; Seidlitz, E.P.; Singh, G. Glutamate signaling in healthy and diseased bone. *Front. Endocrinol.* **2012**, *3*. [[CrossRef](#)] [[PubMed](#)]
93. Kalariti, N.; Lembessis, P.; Koutsilieris, M. Characterization of the glutamatergic system in MG-63 osteoblast-like osteosarcoma cells. *Anticancer Res.* **2004**, *24*, 3923–3929. [[PubMed](#)]
94. Blum, R.; Konnerth, A. Neurotrophin-mediated rapid signaling in the central nervous system: Mechanisms and functions. *Physiology* **2005**, *20*, 70–78. [[CrossRef](#)] [[PubMed](#)]
95. Jie-Li, L.; Bin, C.; Li, Q.; Xiao-Ying, L.; Lian-Fu, D.; Guang, N.; Jian-Min, L. NMDA enhances stretching-induced differentiation of osteoblasts through the ERK1/2 signaling pathway. *Bone* **2008**, *43*, 469–475.
96. Bhangu, P.S.; Genever, P.G.; Spencer, G.J.; Grewal, T.S.; Skerry, T.M. Evidence for targeted vesicular glutamate exocytosis in osteoblasts. *Bone* **2001**, *29*, 16–23. [[CrossRef](#)]
97. Zhou, X.; Wei, J.; Song, M.; Francis, K.; Yu, S.P. Novel role of KCNQ2/3 channels in regulating neuronal cell viability. *Cell. Death Differ.* **2011**, *18*, 493–505. [[CrossRef](#)] [[PubMed](#)]
98. Kihara, T.; Hirose, M.; Oshima, A.; Ohgushi, H. Exogenous type I collagen facilitates osteogenic differentiation and acts as a substrate for mineralization of rat marrow mesenchymal stem cells *in vitro*. *Biochem. Biophys. Res. Commun.* **2006**, *341*, 1029–1035. [[CrossRef](#)] [[PubMed](#)]
99. Mizuno, M.; Kuboki, Y. Osteoblast-related gene expression of bone marrow cells during the osteoblastic differentiation induced by type I collagen. *J. Biochem.* **2001**, *129*, 133–138. [[CrossRef](#)] [[PubMed](#)]
100. Salaszyk, R.M.; Williams, W.A.; Boskey, A.; Batorsky, A.; Plopper, G.E. Adhesion to vitronectin and collagen I promotes osteogenic differentiation of human mesenchymal stem cells. *J. Biomed. Biotechnol.* **2004**, *2004*, 24–34. [[CrossRef](#)] [[PubMed](#)]
101. Viguet-Carrin, S.; Garnero, P.; Delmas, P.D. The role of collagen in bone strength. *Osteoporos. Int.* **2006**, *17*, 319–336. [[CrossRef](#)] [[PubMed](#)]
102. Mathews, S.; Bhonde, R.; Gupta, P.K.; Totey, S. A novel tripolymer coating demonstrating the synergistic effect of chitosan, collagen type I and hyaluronic acid on osteogenic differentiation of human bone marrow derived mesenchymal stem cells. *Biochem. Biophys. Res. Commun.* **2011**, *414*, 270–276. [[CrossRef](#)] [[PubMed](#)]
103. Gajko-Galicka, A. Mutations in type I collagen genes resulting in osteogenesis imperfecta in humans. *Acta Biochim. Pol.* **2002**, *49*, 433–441. [[PubMed](#)]
104. Basel, D.; Steiner, R.D. Osteogenesis imperfecta: Recent findings shed new light on this once well-understood condition. *Genet. Med.* **2009**, *11*, 375–385. [[CrossRef](#)] [[PubMed](#)]
105. Desiderio, V.; Tirino, V.; Papaccio, G.; Paino, F. Bone defects: Molecular and cellular therapeutic targets. *Int. J. Biochem. Cell. Biol.* **2014**, *51*, 75–78. [[CrossRef](#)] [[PubMed](#)]
106. Maraka, S.; Kennel, K.A. Bisphosphonates for the prevention and treatment of osteoporosis. *BMJ* **2015**, *351*, h3783. [[CrossRef](#)] [[PubMed](#)]
107. Drake, M.T.; Clarke, B.L.; Khosla, S. Bisphosphonates: Mechanism of action and role in clinical practice. *Mayo Clin. Proc.* **2008**, *83*, 1032–1045. [[CrossRef](#)] [[PubMed](#)]
108. Komarova, S.V.; Dixon, S.J.; Sims, S.M. Osteoclast ion channels: Potential targets for antiresorptive drugs. *Curr. Pharm. Des.* **2001**, *7*, 637–654. [[CrossRef](#)] [[PubMed](#)]
109. Nardone, V.; D'Asta, F.; Brandi, M.L. Pharmacological management of osteogenesis. *Clinics* **2014**, *69*, 438–446. [[CrossRef](#)]
110. Davies, G.C.; Huster, W.J.; Lu, Y.; Plouffe, L., Jr.; Lakshmanan, M. Adverse events reported by postmenopausal women in controlled trials with raloxifene. *Obstet. Gynecol.* **1999**, *93*, 558–565. [[CrossRef](#)] [[PubMed](#)]
111. Wimalawansa, S.J. Long- and short-term side effects and safety of calcitonin in man: A prospective study. *Calcif. Tissue Int.* **1993**, *52*, 90–93. [[CrossRef](#)] [[PubMed](#)]
112. Acevedo, C.; Bale, H.; Gludovatz, B.; Wat, A.; Tang, S.Y.; Wang, M.; Busse, B.; Zimmermann, E.A.; Schaible, E.; Allen, M.R.; *et al.* Alendronate treatment alters bone tissues at multiple structural levels in healthy canine cortical bone. *Bone* **2015**, *81*, 352–363. [[CrossRef](#)] [[PubMed](#)]
113. Watts, N.B. Long-term risks of bisphosphonate therapy. *Arq. Bras. Endocrinol. Metabol.* **2014**, *58*, 523–529. [[CrossRef](#)] [[PubMed](#)]
114. Demonaco, H.J. Patient- and physician-oriented web sites and drug surveillance: Bisphosphonates and severe bone, joint, and muscle pain. *Arch. Intern. Med.* **2009**, *169*, 1164–1166. [[CrossRef](#)] [[PubMed](#)]

115. Oh, Y.H.; Yoon, C.; Park, S.M. Bisphosphonate use and gastrointestinal tract cancer risk: Meta-analysis of observational studies. *World J. Gastroenterol.* **2012**, *18*, 5779–5788. [[CrossRef](#)] [[PubMed](#)]
116. Andrici, J.; Tio, M.; Eslick, G.D. Meta-analysis: Oral bisphosphonates and the risk of oesophageal cancer. *Aliment. Pharmacol. Ther.* **2012**, *36*, 708–716. [[CrossRef](#)] [[PubMed](#)]



© 2016 by the authors; licensee MDPI, Basel, Switzerland. This article is an open access article distributed under the terms and conditions of the Creative Commons by Attribution (CC-BY) license (<http://creativecommons.org/licenses/by/4.0/>).